

Response to comments by referee 1

We would like to thank you for your comments and helpful suggestions. We revised our manuscript according to these comments and suggestions.

Specific comments:

This paper characterizes mixing layer height (MLH) over the major cities in the North China Plain based on the two-year surface observations. The relationship between MLH and regional air pollution is explored using concurrent PM, MLH, surface radiation, and meteorological parameters in the same cities. Overall, the paper is well written and the finding about the low MLH in southern Hebei is valuable to develop an efficient air pollution mitigation strategy in North China. I suggest the paper should be accepted by ACP after the authors address my comments below.

Comment 1:

It is not clear what is the difference between the MLH discussed here and the traditional defined planetary boundary layer height (PBLH). It would be interesting to see if the MLH obtained from surface can be inter-compared with PBLH from soundings like Guo J. et al. (2016).

Response 1:

Thank you for your helpful suggestion. Actually, we have already made comparisons between the MLH obtained from ceilometers and sounding data in Tang et al. (2016). The comparison results found that the ceilometers underestimate the MLH under conditions of neutral stratification caused by strong winds, whereas it overestimates MLH when sand-dust is crossing. When we excluded these two special weather conditions, the ceilometers observation results were fairly consistent with those retrieved from the sounding data. In addition, since the ceilometers can reflect the rainy conditions and precipitation will influence the MLH retrieval, data for precipitation were also excluded. In our study, data rectifications were made at the BJ, SJZ, TJ and QHD stations. The criterion to exclude these data points is as follows: (a) precipitation, i.e., a cloud base lower than 4000 m and the attenuated backscattering coefficient of at least $2 \times 10^{-6} \text{ m}^{-1} \text{ sr}^{-1}$ within 0 m and the cloud base, (b) sandstorm, i.e., the ratio of $\text{PM}_{2.5}$ to PM_{10} suddenly decreased to 30 % or lower and the PM_{10} concentration was higher than $500 \mu\text{g m}^{-3}$, and (c) strong winds, i.e., a sudden change in temperature and wind speed when cold fronts passed by (Muñoz and Undurraga, 2010; Tang et al., 2016; Kamp and McKendry, 2010). Relevant contents were modified in section 2.2 in the revised manuscript.

Comment 2:

L266, the authors attribute the lower summertime MLH in QHD to the higher frequency of sea breeze. However, the underlying physical mechanism is not fully explained. Intuitively, the active sea breezes should come with more unstable atmosphere over the land. Figure 5 about prevailing wind directions in different seasons is referred, but it is still unclear to me how this figure supports the hypothesis above. Some detailed discussions are needed to better describe the formation and

characteristics of the sea breeze in the coastal regions.

Response 2:

Thank you for your helpful suggestion. We are sorry for the unclear illustration about the impact of sea breezes. Here, we re-created the monthly diurnal wind vectors as shown below in Fig.1. We can see that the sea breeze usually started at midday (approximately 11:00 LT) and prevailed during daytime at the QHD station in spring and summer (Fig. 1d). The sea breeze usually brings a cold and stable air mass from the sea to the coastal region. Under the influence of the abrupt change of aerodynamic roughness and temperature between the land and sea surfaces, a thermal internal boundary layer (TIBL) will form in the coastal areas. Then, the local mixing layer will be replaced by the TIBL. Under the influence of warm air on land, the sea air advects downwind and warms, leading to a weak temperature difference between the air and the ground. In consequence, the TIBL warms less rapidly due to the decreased heat flux at the ground, and the rise rate is reduced. In addition, since the TIBL deepens with distance downwind and usually can not extend all the way to the top of the intruding marine air, the remaining cool marine air above the TIBL will hinder the TIBL vertical development (Stull, 1988; Sicard et al., 2006). As a result, the MLH at the QHD station was lower than other stations from April to September. Since the south-southwesterly wind impacts were enhanced in summer due to the weak synoptic systems, a frequent occurrence of the TIBL resulted in the lowest MLH at the QHD station in summer. To better illustrate the sea breeze impacts, we also made relevant modifications in section 4.1 in the revised manuscript.

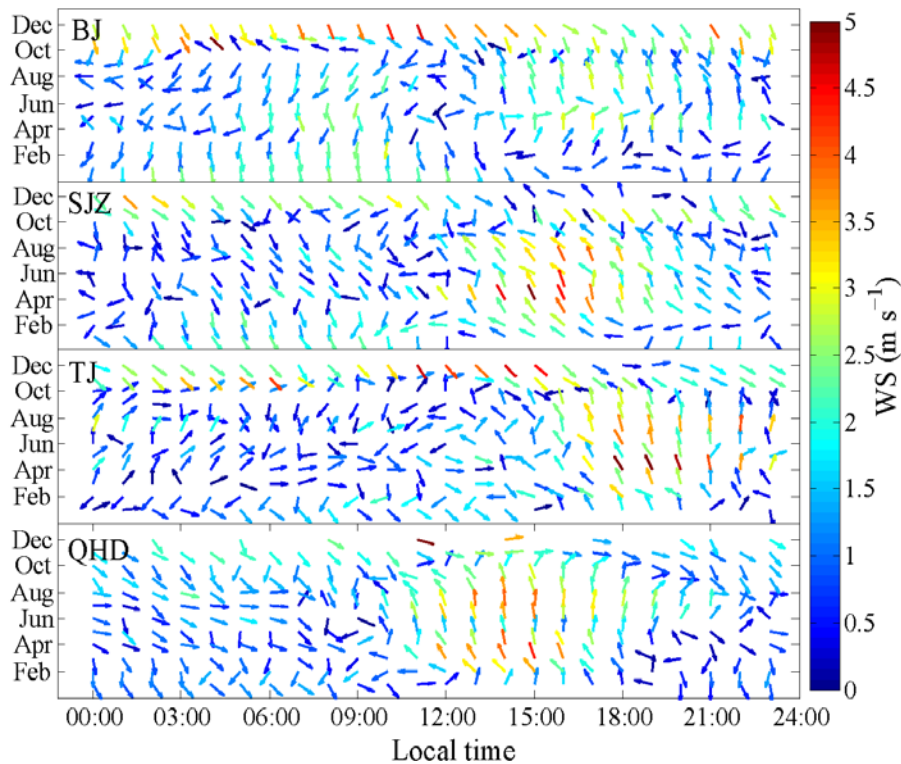


Fig. 1 Monthly variations of diurnal wind vectors at the BJ, SJZ, TJ and QHD stations from December 2013 to November 2014.

Comment 3:

L372, to overcome the lack of radio sounding in SJZ, how about directly using the reanalysis data? The quality of reanalysis can be evaluated by radio-sound at XT.

Response 3:

Thank you for your suggestion. We have made comparisons between reanalysis data and observation data at the Xingtai (XT) and Laoting (LT) stations, respectively. The reanalysis data were downloaded from the ECMWF website (<http://apps.ecmwf.int/datasets/data/interim-full-mnth/levtype=pl/>). As shown in Fig.2, there were large discrepancies between the two data sets. Meanwhile, the vertical resolution of the reanalysis data was too low to calculate the wind shear profile. Therefore, the reanalysis data could not be used to describe the meteorological parameter variations in this study. Considering the absence of vertical meteorological observations in other stations, comparisons of wind speed between the XT and Shijiazhuang (SJZ) stations, as well as LT and Qinhuangdao (QHD) stations were also made with the reanalysis data (Fig. 3). The wind speed between the XT and SJZ stations, and the LT and QHD stations were highly correlated, respectively, which indicated that the wind speeds in SJZ and QHD could be replaced by data in the XT and LT stations, respectively.

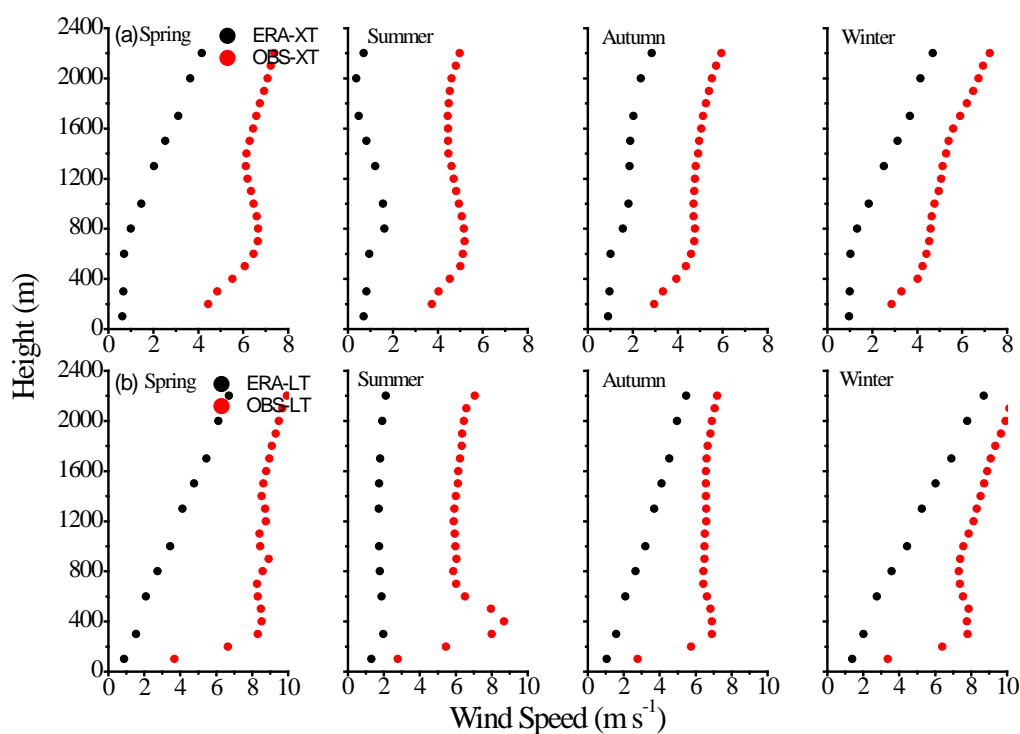


Fig. 2 Comparisons of seasonal wind speed profiles between the reanalysis and observation data at (a) the XT stations and (b) the LT stations.

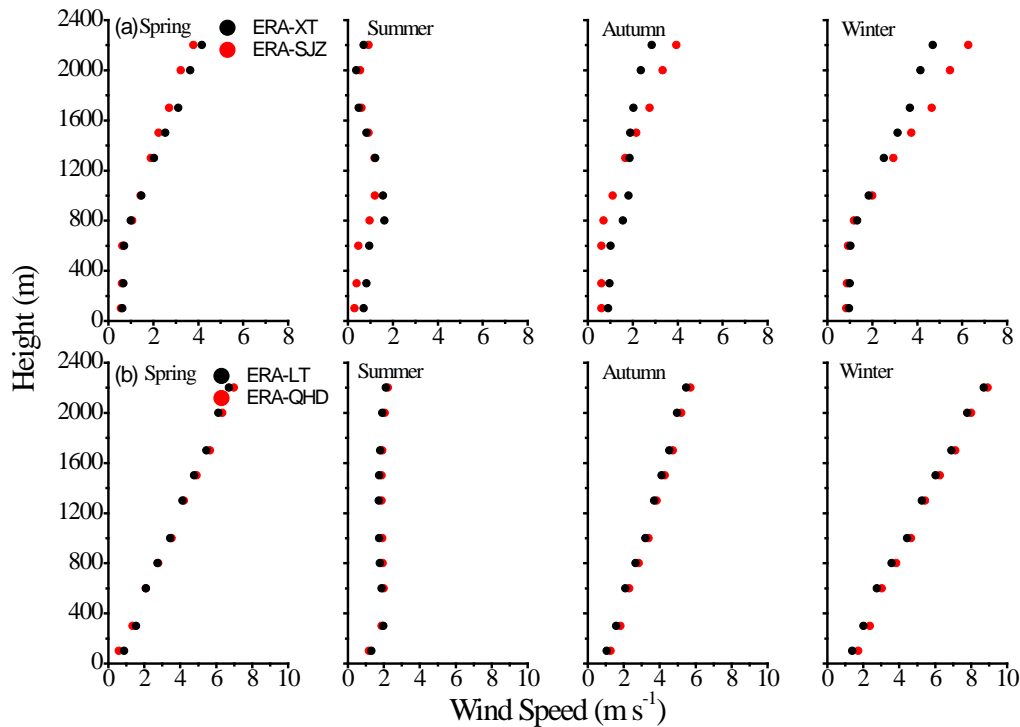


Fig. 3 Comparisons of seasonal wind speed profiles between the (a) XT and SJZ stations and the (b) LT and QHD stations with reanalysis data.

Comment 4:

Section 4.1, could absorbing aerosols be another factor to explain the reason of the low MLH in southern Hebei? Observations have revealed that the ambient aerosols can become highly absorptive in the urban conditions in China [Peng J. et al., 2016, PNAS]. The strong solar absorption near the top of PBL can increase the atmospheric stability and convective inhibition energy [Wang Y. et al., 2013, AE; Li Z. et al., 2016, Rev. Geos.]. Those possible influences from the feedback of air pollution should be discussed and quantified if possible.

Response 4:

Thank you for your constructive suggestion very much. We have read your mentioned papers and some other relevant research. Absorbing aerosols above the MLH can be another factor affecting the MLH because it gives rise to an increasing temperature aloft but a decreasing temperature at the surface, which will enhance the strength of capping inversion and inhibit the convective ability (Peng et al., 2016; Wang et al., 2013; Li et al., 2016). In contrast, absorbing aerosols within the mixing layer could reduce the capping inversion intensity despite the reduction in the surface buoyancy flux and raise the MLH (Yu et al., 2002). Considering the higher concentrations of surface $PM_{2.5}$ in southern Hebei, absorbing aerosols could likely have some impacts on MLH development. However, the comprehensive influences from the feedback of absorbing aerosols above and below the MLH are difficult to explain without sufficient knowledge of the vertical variations in absorbing aerosols. Although the near-ground absorbing aerosol concentration (such as black carbon) has regional differences (Zhao et al., 2013), the absorbing aerosol column concentrations could be

consistent (Gong et al., 2017) with little difference in absorptive aerosol optical depths (AAOD). In addition, the mixed state and morphology of absorbing aerosols dominate the absorption effects (Jacobson, 2001; Bond et al., 2013). Therefore, without sufficient observation data, it is difficult to discuss and quantify the possible influences from the feedback of air pollution on the MLH development at present. Some elaborate experiments of vertical profiles and morphology need to be implemented in future studies. To compensate for this deficiency and inform readers of the uncertainties, the relevant contents were modified in section 4.2 in the revised manuscript.

Comment 5:

L437, what makes the RH at SJZ is higher than that in BJ and TJ? SJZ is more inland than those two cities.

Response 5:

Thank you for your suggestion. As shown in Fig. 4, seasonal distributions of near-ground RH from December 2013 to November 2014 in the NCP were depicted below. It was obvious that southern Hebei had higher RH than that in the northern NCP. The RH distribution was not only related to the distance from the sea but also to the flow fields and synoptic systems. This might result from the frequent passage of the Siberian High in the northern NCP, especially in spring and winter. In spring, when frequent sand storms occur, a dry air mass is brought to the northern NCP; thus the RH in the northern NCP was far less than that in southern Hebei (Fig. 4a). Meanwhile, under the impact of the Siberian High, a frequent weak northwest flow from Inner Mongolia will bring cold and dry air to the northern NCP in winter and autumn, and such north flow was too weak to reach southern Hebei (Su et al., 2004), which will lead to a lower RH in the northern NCP (Fig. 4c and 4d). In addition, the higher RH in southern Hebei could also be affected by the subtropical high (wet southeast flow) from the Yellow Sea.

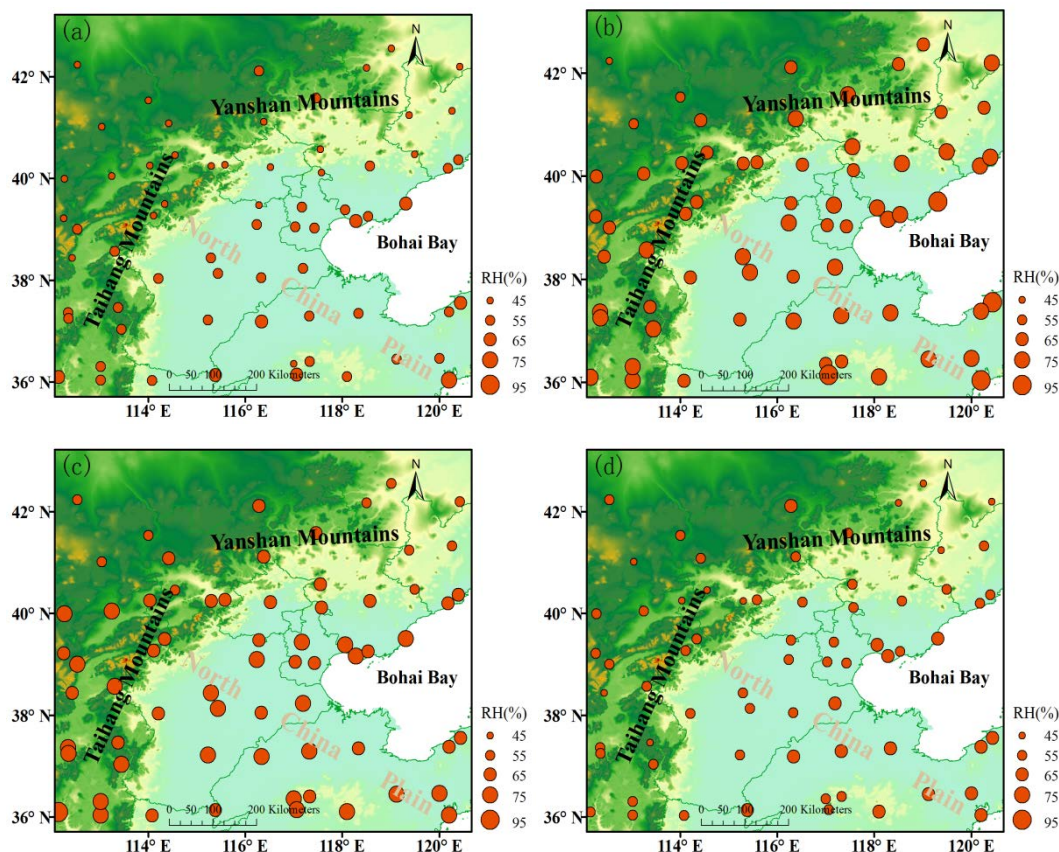


Fig. 4 Distributions of seasonal averaged RH in the NCP from December 2013 to November 2014: (a) spring, (b) summer, (c) autumn and (d) winter.

Comment 6:

L432-445, some basics of new particle formation in urban condition should be thoroughly reviewed. Please refer to Zhang, R. 2010, Science and 2015, Rev. Chem.

Response 6:

Thank you for your helpful suggestion. We apologize for our superficial understanding of the new particle formation and growth processes. We re-created some figures to illustrate the annual means of RH and T distributions over north China (Fig. 5). The T value in southern Hebei was similar to that in the northern NCP (Fig. 5a), which indicated an almost consistent temperature condition for an atmospheric chemical reaction between these two areas (Seinfeld J. and S. Pandis, 1998; Zhang et al., 2010; Zhang et al., 2015). However, differences existed in RH between southern Hebei and the northern NCP. The RH in southern Hebei was always higher than that in the northern NCP (Fig. 5b). As mentioned in our response to your comment 5, the Siberian and the subtropical high will be responsible for this RH distribution in the NCP region. Since the RH is a key factor for haze development, higher RH is beneficial to fine particle growth through the hygroscopic growth process and heterogeneous reaction. Relevant contents were modified in section 4.3.1 in the revised manuscript.

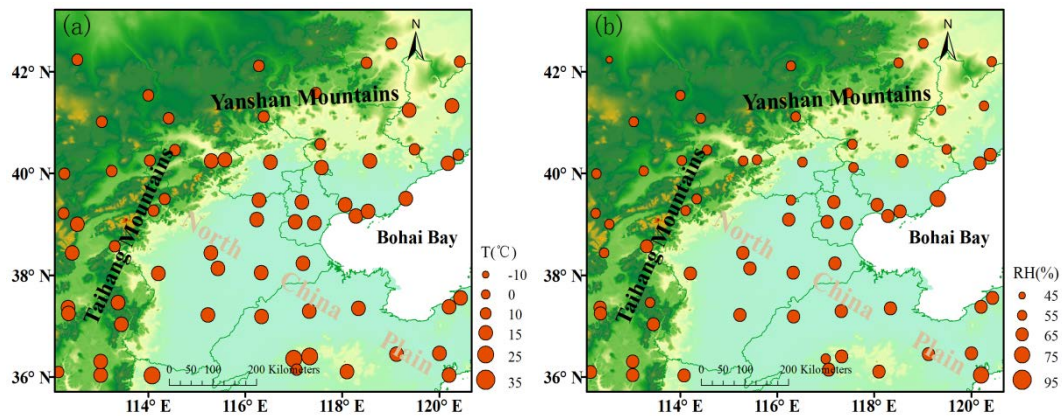


Fig. 5 Distributions of annual means of (a) T and (b) RH over the NCP region from December 2013 to November 2014.

Comment 7:

Fig. 8. Define V_c in the figure caption.

Response 7:

Thank you for your suggestion. We have already added the definition for V_c in the figure caption of Fig. 9 in the revised manuscript.

References:

- Bond, T., S. Doherty, D. Fahery et al.: Bounding the role of black carbon in the climate system: a scientific assessment, *J. Geophys. Res.*, 118, 1-173, doi:10.1002/jgrd.50171, 2013.
- Gong, C., J. Xin, S. Wang, Y. Wang, T. Zhang: Anthropogenic aerosol optical and radiative properties in the typical urban/suburban regions in China, *Atmos. Res.*, doi:10.1016/j.atmosres.2017.07.002, 2017.
- Jacobson, M.: Strong radiative heating due to the mixing state of black carbon in atmospheric aerosols, *Nature*, 409,695-697, 2001.
- Li, Z., W. Lau, and V. Ramanathan et al.: Aerosol and monsoon climate interactions over Asia, *Rev. Geophys.*, 54, 886-929, doi:10.1002/2015RG000500, 2016.
- Muñoz, R. and A. Undurraga: Daytime Mixing layer over the Santiago Basin: Description of Two Years of Observations with a Lidar Ceilometer, *J. Appl. Meteorol. Clim.*, 49(8), 1728-1741, doi:10.1175/2010jamc2347.1, 2010.
- Peng, J., M. Hu, S. Guo, Z. Du, J. Zheng, D. Shang, M. L. Zamora, L. Zeng, M. Shao, Y. Wu, J. Zheng, Y. Wang, C. R. Glen, D. R. Collins, M. J. Molina, and R. Zhang: Markedly enhanced absorption and direct radiative forcing of black carbon under polluted urban environments, *P. Natl. Acad. Sci. Usa.*, 113(4266-4271), doi:10.1073/pnas.1602310113, 2016.
- Seinfeld J. and S. Pandis: *Atmospheric Chemistry and Physics: From Air Pollution to Climate Change*, New York: John Wiley and Sons, 1998.
- Sicard, M., C. Pérez, F. Roca-denbosch, J. Baldasano, and D. García-Vizcaino:

- Mixed-Layer Depth Determination in the Barcelona Coastal Area From Regular Lidar Measurements: Methods, Results and Limitations. *Boundary-Layer Meteorology* 119, 135-157, 2006.
- Stull, R.: An Introduction to Boundary Layer Meteorology, Kluwer Academic Publishers, Dordrecht, 1988.
- Su, F., M. Yang, J. Zhong, Z. Zhang: The effects of synoptic type on regional atmospheric contamination in North China, *Res. Of Environ. Sci.*, 17(3), doi:10.13198/j.res.2004.03.18.sufq.006, 2004.
- Tang, G., J. Zhang, X. Zhu, T. Song, C. Munkel, B. Hu, K. Schäfer, Z. Liu, J. Zhang, L. Wang, J. Xin, P. Suppan, and Y. Wang, Mixing layer height and its implications for air pollution over Beijing, China, *Atmospheric Chemistry and Physics*, 16, 2459-2475, doi:10.5194/acp-16-2459-2016, 2016.
- Kamp, V., and I. McKendry: Diurnal and Seasonal Trends in Convective Mixed-Layer Heights Estimated from Two Years of Continuous Ceilometer Observations in Vancouver, BC, *Bound.-Lay. Meteorol.*, 137(3), 459-475, doi:10.1007/s10546-010-9535-7, 2010.
- Wang, Y., M. Zamora, and R. Zhang: New Directions: Light absorbing aerosols and their atmospheric impacts, *Atmos. Environ.*, 81, 713-715, doi: 10.1016/j.atmosenv.2013.09.034, 2013.
- Wei, J., G. Tang, X. Zhu, L. Wang, Z. Liu, M. Cheng, C. Munkel, X. Li and Y. Wang: Thermal internal boundary layer and its effects on air pollutants during summer in a coastal city in North China, *Journal of Environmental Sciences*, 1001-0742, doi:10.1016/j.jes.2017.11.006, 2017.
- Yu, H., S. Liu, and R. Dickinson: Radiative effects of aerosols on the evolution of the atmospheric boundary layer, *J. Geo. Res.: Atmos.*, 107, D12(4142), doi:10.1029/2001JD000754, 2002.
- Zhang, R., G. Hui, S. Guo, M. Zamora, Q. Ying, Y. Lin, W. Wang, M. Hu, and Y. Wang: Formation of Urban Fine Particulate Matter, *Chem. Rev.*, 115, 3803-3855, doi: 10.1021/acs.chemrev.5b00067, 2015.
- Zhang, R.: Getting to the Critical Nucleus of Aerosol Formation, *Science*, 328(5984), 1366-1367, doi: 10.1126/science.1189732, 2010.
- Zhao, P., F. Dong, Y. Yang, D. He, X. Zhao, W. Zhang, Q. Yao, and H. Liu: Characteristics of carbonaceous aerosol in the region of Beijing, Tianjin, and Hebei, China, *Atmos. Environ.*, 71, 389-398, doi: 10.1016/j.atmosenv.2013.02.010, 2013.

Response to comments by referee 2

We would like to thank you for your comments and helpful suggestions. We revised our manuscript according to these comments and suggestions.

Specific comments:

This study reveals the spatial variation of mixing layer height (MLH) over northern China plain (NCP) based on a two-year measurement at four primary cities with different geographic allocation across NCP. The authors attribute the different spatial pattern of MLH between southern Hebei and northern NCP to the distinct wind shear features between the two interested regions. The analysis on the long-term measurement of MLH in this study provides a meaningful insight on the climatological features of boundary layer condition during the haze episodes over NCP. Also, the discussions about the associations of MLH and other meteorological factors with the near-ground particle pollution are sufficiently presented in this work. However, the following concerns should be addressed before publication.

Comment 1:

Considering the possible strong aerosol-radiation interaction because of the heavily pollution, the surface net radiation is supposed to be lower over the regions with more heavily pollution because of the strong scattering and/or absorbing of solar radiation by aerosols. However, in this study, though the near-ground PM_{2.5} concentration over southern Hebei is 1.3 times higher than that of north China plain (NCP), there is no significant difference in the net radiation at Shijiazhuang (SJZ) located southern Hebei from at Beijing (BJ) located over NCP. One probable reason is because the aerosol optical depth (AOD) over the two sites was comparable, leading to comparable capacity reducing solar radiation. The authors may check the AOD data to obtain a convinced explanation for why the net radiation is spatial consistent, given the presence of aerosol-radiation interaction.

Response 1:

Thank you for your helpful suggestion. We have checked the AOD distribution in the NCP as you suggested. The AOD data were retrieved with the dark target algorithm from the Moderate Resolution Imaging Spectra-radiometer (MODIS) aerosol products on board the NASA EOS (Earth observing system) Terra satellite. As shown in Fig. 1 below, the AOD in Shijiazhuang (SJZ) was 1.1 and 1.0 times higher than that at the Beijing (BJ) and Tianjin (TJ) stations, respectively. Given the presence of aerosol-radiation interaction, the comparative amount of AOD could be one probable reason to explain the nearly consistent net radiation between the SJZ and BJ stations. In our revised manuscript, the net radiation analysis was replaced by gradient Richardson number (Ri) studies, and Ri is a better index that can evaluate the atmospheric stability from both the perspectives of thermal and mechanism forces. Then, the low mixing layer height (MLH) in winter in southern Hebei mainly resulted from the stable turbulent stratification (using summer and winter as examples) (Fig.1). Relevant contents were modified in section 4.2 in the revised manuscript. In addition, we discovered some new findings when the AOD analysis was added in the

discussion. Please refer to comment 2.

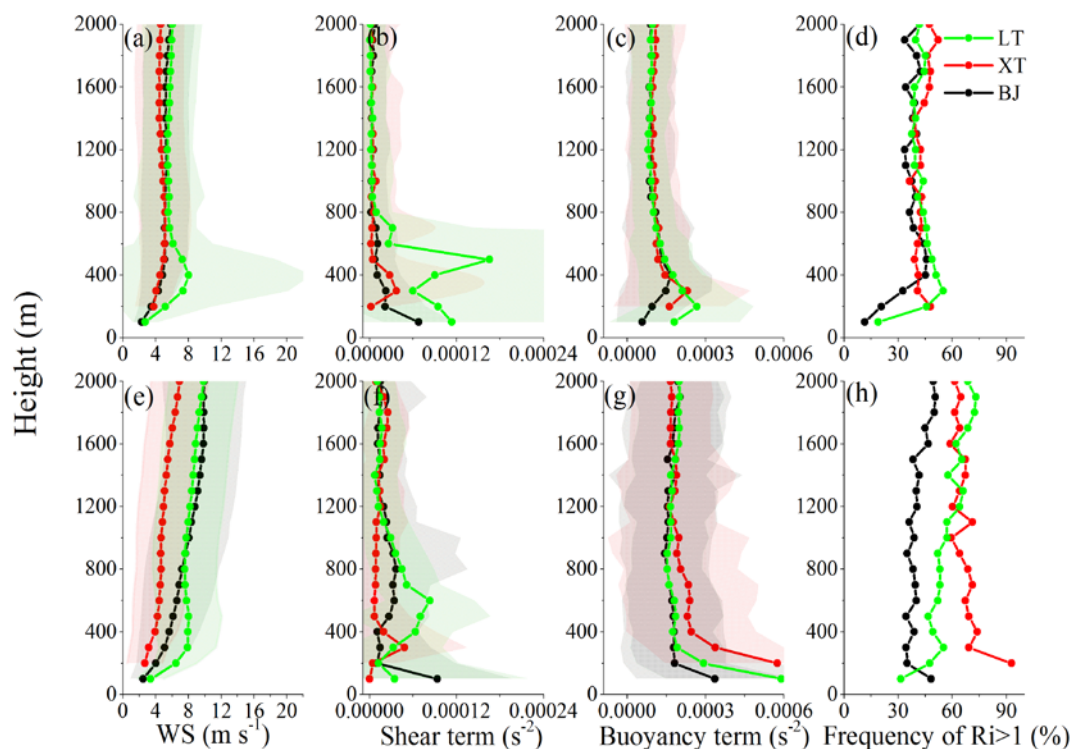


Fig.1 Vertical profiles of (a, e) the horizontal WS, (b, f) the shear term, (c, g) the buoyancy term and (d, h) the percentage of $Ri > 1$ at the BJ, XT and LT stations in summer (upper panel) and winter (lower panel).

Comment 2:

In addition to the difference in mixing layer height (MLH), how likely does the spatial variation in pollutant emissions contribute to the difference in the near-ground PM pollution between SJZ and BJ?

Response 2:

Thank you for your suggestion. Since the particle has direct emission sources and secondary sources, and the distribution of direct emissions cannot represent the total contribution of emissions to the particle concentration. The near-ground PM_{2.5} concentration could represent the particle concentrations at the ground, but considering that the particle lifetime is much longer than that of trace gases, the particle concentrations are nearly uniform in the mixing layer because of the strong vertical mixing. Therefore, near-ground PM_{2.5} concentrations cannot be used to evaluate the emissions influences between different regions if the mixing layer heights are different. AOD, which represents the aerosol column concentration, is a much better indicator for the emissions difference. As shown in Fig. 2, the major sites in southern Hebei (the SJZ, Handan (HD) and Xingtai (XT) stations) and the northern NCP (the BJ and TJ stations) were enclosed with white rectangles. The average AOD value at the southern Hebei stations was 1.2 times higher than the AOD at the northern NCP regions, while the near-ground PM_{2.5} concentration in southern Hebei was 1.5 times higher than that in the northern NCP. If the AOD difference represents the emission discrepancy, the remaining differences of PM_{2.5} concentration may be

induced by the meteorology. In other words, except for the emission effect, the meteorological conditions also play an important role in pollutant contrast between these two areas. Relevant contents were also modified in section 4.3 in our revised manuscript.

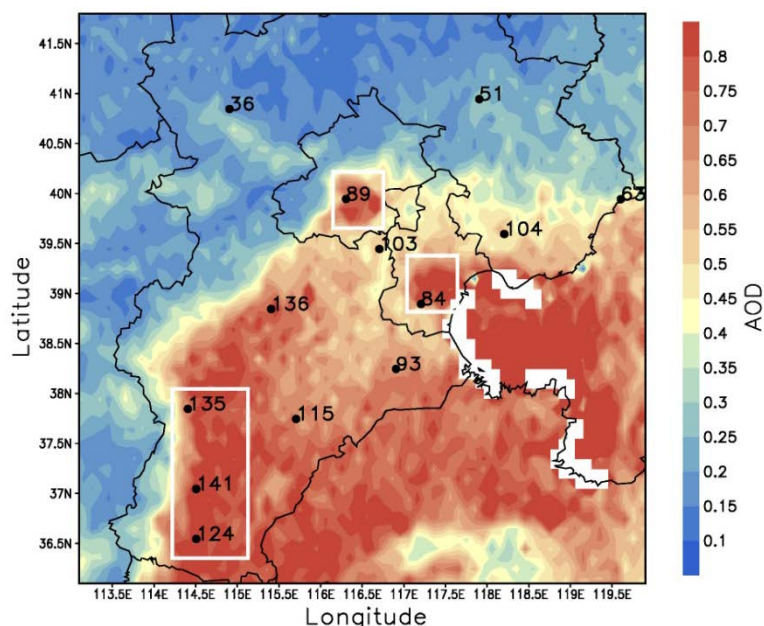


Fig. 2 AOD distribution from December 2013 to November 2014 in the NCP. The PM_{2.5} concentrations of the 13 observation sites were also marked beside each station. Major sites in the northern NCP (BJ and TJ) and southern Hebei (SJZ, XT and HD) were enclosed by white rectangles.

Comment 3:

The authors attribute the spatial difference in wind shear over NCP during winter to the influence of front passing associated with the Siberian High (lines 403-405). Is the front also the dominant control of the relative humidity over NCP during winter? Is there any other reason leading to the discrepancy in relative humidity between the two regions in question?

Response 3:

The spatial difference in wind shear over the NCP in spring, autumn and winter probably resulted from the more frequent weak cold air impact on the northern NCP region. When the cold air was brought by a high-pressure system, the cold front formed and enhanced the wind shear in BJ. However, in summer, due to the northward lift and westward intrusion of the subtropical high on the NCP, the diminished effect of the weak cold air on the northern NCP accompanied with strong solar radiation and turbulent activities will lead to less wind shear contrast in the vertical direction between southern Hebei and the northern NCP. Certainly, the front is also the dominant control of the RH over the NCP. In addition, higher RH in southern Hebei might result from the frequent passage of the Siberian High in the north NCP, especially in spring and winter. In spring, when frequent sand storms occur, a dry air mass is brought to the northern NCP; thus, the RH in the northern NCP was far less

than that in southern Hebei (Fig. 3a). Meanwhile, under the impact of the Siberian High, a frequent weak northwest flow from Inner Mongolia will bring cold and dry air to the northern NCP in winter and autumn, and such north flow was usually too weak to reach southern Hebei (Su et al., 2004), which will lead to lower RH in the northern NCP (Figs. 3c and 3d). In addition, the higher RH in southern Hebei could also be affected by the subtropical high (wet southeast flow from the Yellow Sea).

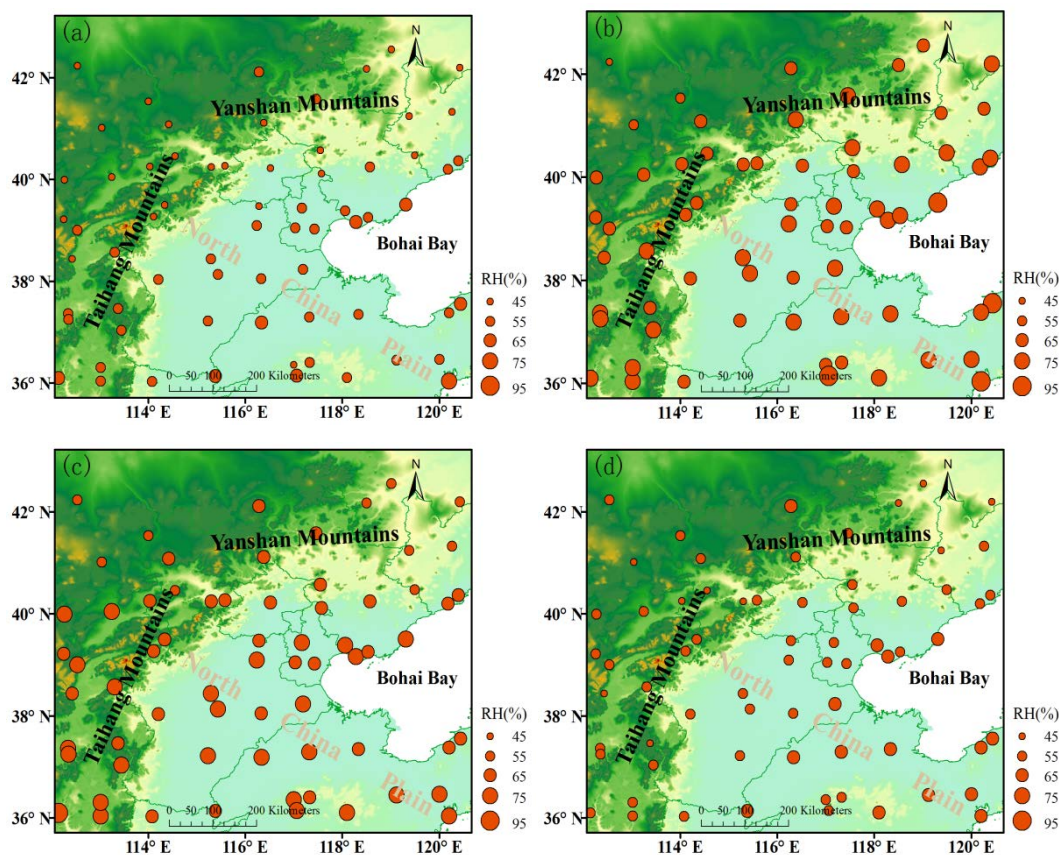


Fig. 3 Distributions of seasonal averaged RH in the NCP from December 2013 to November 2014: (a) spring, (b) summer, (c) autumn and (d) winter.

Comment 4:

Given that both Tianjin (TJ) and Qinhuangdao (QHD) are located at coastal region and suffering highly frequent sea breezes during summer (Fig. 5), why the MLH of TJ is much higher than the case in QHD, since the relatively low MLH in QHD is attributed by the authors to the intensive occurrence of sea breeze during summer (lines 265-266)?

Response 4:

Thank you for your suggestion, and we apologize for our unclear description. Actually, the MLH at the coastal region was affected by the thermal internal boundary layer (TIBL), not the sea breeze. When the cold air mass came with the sea breeze and the top of the mixing layer was higher than the top of the air mass, the TIBL will form within the original mixing layer, interrupting the original mixing layer development and decreasing the MLH. With distance inland, the top of the sea air mass will enhance and exceed the local MLH; if so, the TIBL will not form, and the TIBL

impact will be impaired with distance inland (Stull, 1988). Since the QHD station was only 2 km away from the coastline and the distance of the TJ station was approximately 50 km out to sea, the TIBL will not form in the TJ station. The MLH variation for TJ was the same with those inland sites (BJ and SJZ). The relevant contents were modified in section 4.1 in our revised manuscript.

Technical comments:

Comment 1:

Fig. 7: the unit for the wind shear should be $\text{m s}^{-1} \text{km}^{-1}$.

Response 1:

Since the wind shear = $\sqrt{\left(\frac{\Delta \bar{u}}{\Delta z}\right)^2 + \left(\frac{\Delta \bar{v}}{\Delta z}\right)^2}$ and the unit of wind speed and Δz was m s^{-1} and m , respectively, the unit of wind shear was $\text{m s}^{-1} \text{m}^{-1}$. The study of wind shear was replaced by the study of shear term $\left(\left(\frac{\Delta \bar{u}}{\Delta z}\right)^2 + \left(\frac{\Delta \bar{v}}{\Delta z}\right)^2\right)$ in our revised manuscript. And to be consistent with the unit of buoyancy term, the unit of shear term was s^{-2} .

Comment 2:

The descriptions on Figs. 5c and 5d in lines 320-322 seems not consistent with what was shown in figure. For example, the prevailed wind direction during spring and summer for TJ is southerly as shown in Fig. 5c, which is not the case stated by the text in lines 320-322, i.e. easterly wind is prevailed in TJ.

Response 2:

Thank you for your suggestion, and we have already modified the relevant descriptions in section 4.1 in the revised manuscript.

References:

- Stull, R.: An Introduction to Boundary Layer Meteorology, Kluwer Academic Publishers, Dordrecht, 1988.
- Su, F., M. Yang, J. Zhong and Z. Zhang: The effects of synoptic type on regional atmospheric contamination in North China, Res. Of Environ. Sci., 17(3), doi:10.13198/j.res.2004.03.18.sufq.006, 2004.

Response to short comments

We would like to thank you for your comments and helpful suggestions. We revised our manuscript according to these comments and suggestions.

Specific comments:

The climatology of MLH at four sites over NCP was investigated using long-term measurements. However, lots of statements in the manuscript and part of conclusions were not well supported. Thus, a major revision is suggested.

Comment 1:

LINE 214-215, the definitions of rainy, sandstorm and windy conditions should be given.

Response 1:

Thank you for your suggestion. The criteria to exclude the data points for special conditions are as follows: (a) precipitation, i.e., a cloud base lower than 4000 m and an attenuated backscattering coefficient of at least $2 \times 10^{-6} \text{ m}^{-1} \text{ sr}^{-1}$ within 0 m and the cloud base, (b) sandstorm, i.e., the ratio of $\text{PM}_{2.5}$ to PM_{10} suddenly decreased to 30 % or lower and the PM_{10} concentration was higher than $500 \mu \text{g m}^{-3}$, and (c) strong winds, i.e., a sudden change in temperature and wind speed when cold fronts passed by. We also modified the relevant contents in section 2.2 in the revised manuscript.

Comment 2:

LINE 317-318, “the TJ station was supposed to be an inland site”, the TJ site is quite close to the Bohai sea, which should be considered as a coastal station.

Response 2:

Actually, the Tianjin (TJ) site was set in the courtyard of the Tianjin Meteorological Bureau, which was located south of the urban area (117.20°E , 39.13°N) with approximately 50 km away from the coast. The Qinhuangdao (QHD) station was set up in the Environmental Management College of China (119.57°E , 39.95°N) with only approximately 2 km away from the coastline. Therefore, the TJ site, by contrast, was supposed to be an inland site. In addition, the mixing layer height (MLH) at the coastal region was affected by the thermal internal boundary layer (TIBL), not the sea breeze. When the cold air mass came with the sea breeze and the top of the mixing layer was higher than the top of the air mass, the TIBL will form within the origin mixing layer, interrupt the origin mixing layer development and decrease the MLH. With distance inland, the top of the sea air mass will enhance and exceed the local MLH; if so, the TIBL will not form, and the TIBL impact will be impaired with distance inland (Stull, 1988). Since the QHD station was only 2 km away from the coastline and the distance of the TJ station was approximately 50 km out to sea, the TIBL will not form in the TJ station. The MLH variation for TJ was the same with those inland sites. The relevant contents were modified in section 4.1 in our revised manuscript. From another point of view, the definition of a coastal station should be the one that was affected by the TIBL.

Comment 3:

LINE 319-324, the definition of sea-breeze used in this study should be given. The sea-breeze cannot be identified merely by the near-surface wind speed and direction. How to identify the sea-breeze from background wind? How to calculate the occurrence frequency of sea-breeze at TJ and QHD?

Response 3:

Thank you for your suggestion. The sea-land breeze was a local circulation; it occurs when there is no large scale synoptic system that passes. In our study, we first exclude days with large-scale synoptic systems. Then according to the coastline orientation, if the southeast wind at the TJ station and south and southwest winds at the QHD station occurred at approximately 11:00 LT, and the northwest wind started to blow at approximately 20:00 LT, then this type of circulation was supposed to be a sea-land circulation. The prevailing southeast wind at the TJ station and the south and southwest wind at the QHD station were regarded as sea breezes.

Comment 4:

LINE 326-335, more evidences should be given to support the statement that the movement of sea-breeze suppress the MLH at QHD site in summer. The TJ site also locates in the coastal regions, why the diurnal patterns and seasonal variations of MLH are quite different?

Response 4:

Thank you for your suggestion. Here, we re-created the monthly diurnal wind vectors as shown below in Fig.1. We can see that the sea breeze usually started at midday (approximately 11:00 LT) and prevailed during daytime at the QHD station in spring and summer (Fig. 1d). The sea breeze usually brings a cold and stable air mass from the sea to the coastal region. Under the influence of the abrupt change of aerodynamic roughness and temperature between the land and sea surfaces, a TIBL will form in the coastal areas. Then, the local mixing layer will be replaced by the TIBL. Under the influence of warm air on land, the sea air advects downwind and warms, leading to a weak temperature difference between the air and the ground. In consequence, the TIBL warms less rapidly due to the decreased heat flux at the ground, and the rise rate is reduced. In addition, since the TIBL deepens with distance downwind and usually can not extend all the way to the top of the intruding marine air, the remaining cool marine air above the TIBL will hinder the TIBL vertical development (Stull, 1988; Sicard et al., 2006). As a result, the MLH at the QHD station was lower than other stations from April to September. Since the south-southwesterly wind impacts are enhanced in summer due to the weak synoptic systems, a frequent occurrence of the TIBL resulted in the lowest MLH at the QHD station in summer. As a result, the MLH at the coastal region was affected by the TIBL, not the sea breeze, and the TIBL impact will be impaired with distance inland (Stull, 1988). Since the TJ station was approximately 50 km out to sea, the TIBL will not extend inland so far, and the MLH in TJ had no influence from the TIBL, leading to the same MLH variation with those inland sites (Beijing (BJ) and Shijiazhuang (SJZ)). The relevant contents were modified in section 4.1 in our revised manuscript.

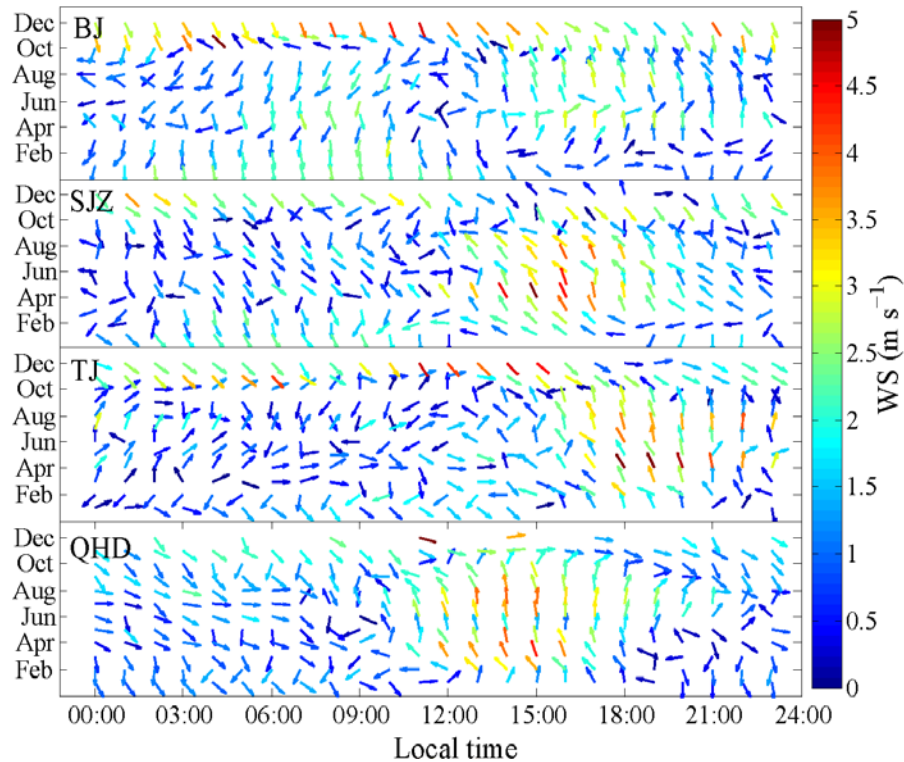


Fig. 1 Monthly variations of prevailing wind at the BJ, SJZ, TJ and QHD stations from December 2013 to November 2014.

Comment 5:

LINE 362-364, the buoyancy fluxes are determined by the surface sensible heat fluxes, not the net radiations. The statements here are inaccurate.

Response 5:

Thank you for your suggestion. The sensible heat fluxes data were not available, so we used net radiation for the analysis. Considering your suggestion, the net radiation analysis was replaced by gradient Richardson number (Ri) studies, and Ri is an index that can evaluate the turbulent stability from both the perspectives of thermal and mechanism forces. Then, the low MLH in southern Hebei mainly resulted from stable turbulent stratification (Fig.2). Relevant contents were modified in section 4.2 in the revised manuscript.

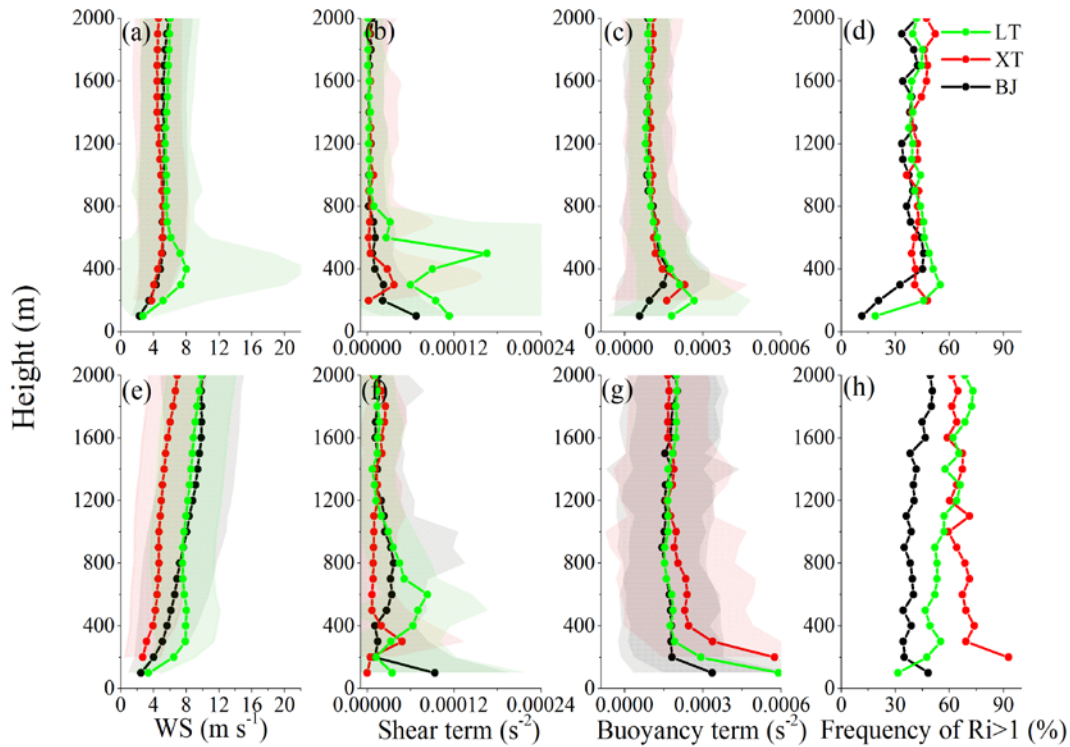


Fig.2 Vertical profiles of (a, e) the horizontal WS, (b, f) the shear term, (c, g) the buoyancy term and (d, h) the percentage of $Ri > 1$ at the BJ, XT and LT stations in summer (upper panel) and winter (lower panel).

Comment 6:

LINE 371-375, before using the sounding data of XT as a replacement of SJZ, the data consistency must be examined and presented, since there are 90 km between these two sites. At least, the general characteristics of MLH at SJZ at 08:00 and 20:00 LT should be well reflected by the sounding data at XT. The data consistency also should be checked between the LT site and QHD site.

Response 6:

Thank you for your suggestion. Since we did not have sounding data at the SJZ and QHD stations, we used the reanalysis data to perform the examination instead. The reanalysis data were downloaded from the ECMWF website (<http://apps.ecmwf.int/datasets/data/interim-full-mnth/levtype=pl/>). Using the wind speed as an example, comparisons of the wind speed between the Xingtai (XT) and SJZ stations and the Laoting (LT) and QHD stations are shown in Fig. 3. The wind speed between the XT and SJZ stations, and the LT and QHD stations were highly correlated, respectively, which indicated that the sounding data in the SJZ and QHD stations could be replaced by data in the XT and LT stations, respectively.

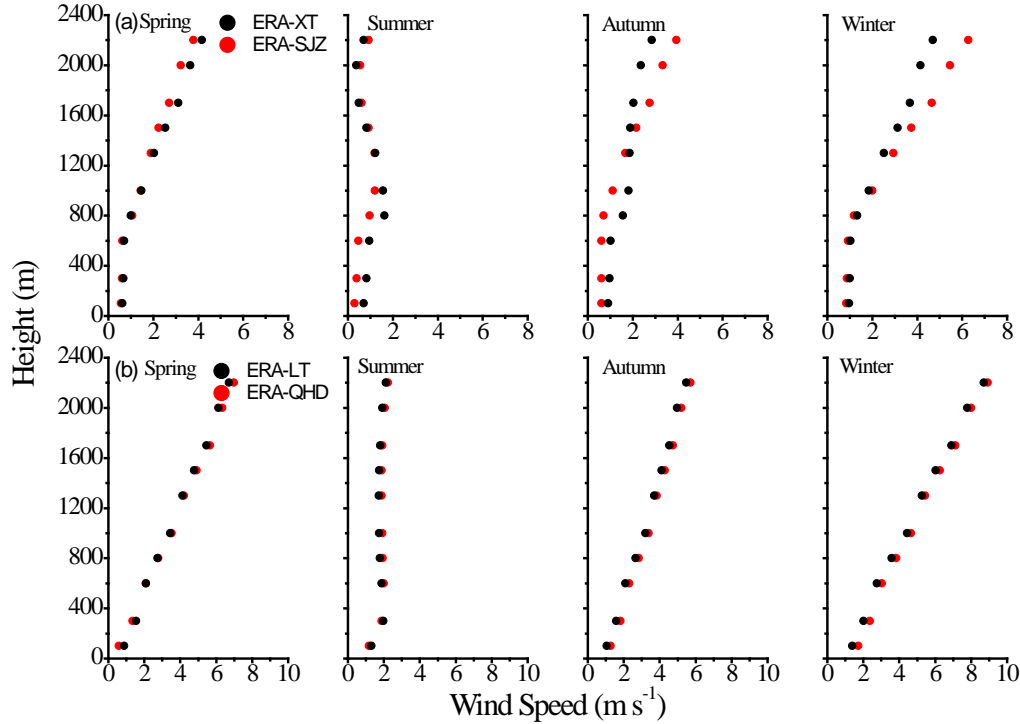


Fig. 3 Comparisons of seasonal wind speed profiles between the (a) XT and SJZ stations and the (b) LT and QHD stations with reanalysis data.

Comment 7:

As shown in Fig. 7, the profiles at XT are almost the same in different season and different moment, which is different from the profiles of other sites. The prevailing wind speed and direction are different in different season, why the profiles are almost the same? The error-bar of the profiles should also be given. In spring and summer, at 20:00 LT there are lots of fluctuations in the profiles at LT, why? Do the terrains play a role in the profiles in different regions?

Response 7:

Although the prevailing wind speed and direction at the XT station were different in different moments and seasons, the vertical variation of each wind speed profile changed slightly. Since the wind shear was defined as the degree of wind speed and direction variation between the upper layer and the lower layer (wind shear =

$$\sqrt{\left(\frac{\Delta \bar{u}}{\Delta z}\right)^2 + \left(\frac{\Delta \bar{v}}{\Delta z}\right)^2},$$

the almost consistent wind shear profiles in different seasons and

different moments indicated a relatively stable atmospheric stratification. Similarly, the stronger variation and higher value of wind shear in the vertical direction at the BJ station suggested a relatively unstable atmospheric stratification, which was probably due to the frequent passage of cold air masses. Fig. 1 shows that the sea breeze changed to land breeze at approximately 20:00 LT; thus, the fluctuations in the profiles at LT could be attributed to the transitory stages of sea-land breeze alternation. Therefore, the terrains certainly play a role in the wind shear profiles in different regions. To further interpret the reasons for low MLH at southern Hebei, we included

an analysis of gradient Richardson number (Ri) profiles at the BJ, XT and LT stations in the revised manuscript and the wind shear study was replaced by the study of shear term $\left(\frac{\Delta \bar{u}}{\Delta z}\right)^2 + \left(\frac{\Delta \bar{v}}{\Delta z}\right)^2$. Since the comparison results at 08:00 LT and 20:00 LT made no difference, we combined the sounding profiles at 08:00 LT and 20:00 LT to make our paper concise and easily understood (Fig. 2). Then, the low MLH in southern Hebei mainly resulted from stable turbulent stratification

Comment 8:

LINE 390-392, the authors merely presented the profiles at 20:00 LT, which cannot support the statement “during the whole night”. More evidences should be given.

Response 8:

Thank you for your suggestion. In our revised manuscript, the meteorological profiles were averaged over 08:00 LT and 20:00 LT, and the shear term and buoyancy term profiles were compared between southern Hebei and the northern NCP (Fig. 2). The wind shear term in southern Hebei was lower than that in the northern NCP within 0-1200 m in spring, autumn and winter, while the buoyancy term was on the opposite, leading to a conclusion that the low MLH in southern Hebei resulted from stable turbulent stratification. In summer, this discrepancy was largely decreased and the MLHs were consistent between these two areas. The relevant contents were modified in section 4.2 in the revised manuscript.

Comment 9:

LINE 404-405, please give evidences to support the statement “the front usually does not reach southern Hebei”.

Comment 10:

LINE 406-408, please give evidences to support the statement “the lessened effects of the front system and strong turbulent exchange will lead to less wind shear contrast in the vertical direction between southern Hebei and the northern NCP.”

Response 9 and 10:

Thank you for your suggestion and we are sorry for our misrepresentation. Although haze evolution in the NCP area is usually regionally consistent, the pollution intensity varies in different regions, which will be partially attributed to the impact of different positions of weather systems. The NCP region is usually influenced by the continental high in the spring, autumn and winter in the lower troposphere. When the high pressure is relatively weak, the northern and southern areas are usually located in front and to the south of the system, respectively. Thus, the weak cold and clean air may be partially responsible for the lighter pollution degree in the northern NCP areas (Su et al., 2004). Meanwhile, the cold front caused by the cold air flow over the northern NCP will enhance the shear term. In summer, due to the northward lift and westward intrusion of the subtropical high on the NCP, the diminished effect of the weak cold air on the northern NCP accompanied with strong solar radiation and turbulent activities will lead to less shear term contrast in the vertical direction between southern Hebei and the northern NCP. Based on this, we have made

modifications in section 4.2 in our revised manuscript.

Comment 11:

LINE 410-419, the authors attribute the high PM concentration in SJZ to the low MLH. It is inaccurate, the different anthropogenic emissions of pollutants in SJZ and BJ should be considered.

Response 11:

Thank you for your suggestion. Since the particle has direct emission sources and secondary sources, the direct emissions distribution cannot represent the total emissions contribution to the particle concentration. The near-ground $PM_{2.5}$ concentration could represent the particle concentrations at the ground, but considering that the lifetime of a particle is much longer than that of trace gases, the particle concentrations are nearly uniform in the mixing layer because of the strong vertical mixing. Therefore, near-ground $PM_{2.5}$ concentrations cannot be used to evaluate the emissions influences between different regions if the mixing layer heights are different. AOD, which represents the aerosol column concentration, is a much better indicator for the emissions difference. In the revised manuscript, we checked the AOD distribution in the NCP to evaluate the emissions effect. The AOD data were retrieved with the dark target algorithm from the Moderate Resolution Imaging Spectra-radiometer (MODIS) aerosol products on board the NASA EOS (Earth observing system) Terra satellite. As shown in Fig. 4, the averaged AOD value at southern Hebei (SJZ, Handan (HD) and Xingtai (XT)) was 1.2 times higher than the AOD at the northern NCP (BJ and TJ) region, while the near-ground $PM_{2.5}$ concentration in southern Hebei was 1.5 times higher than that in the northern NCP. If the difference of AOD represents the emissions discrepancy, the remaining differences of the $PM_{2.5}$ concentration may be induced by the meteorology. In other words, except for the emissions effect, the meteorological conditions also play an important role in pollutant contrast between these two areas. Relevant contents were also modified in section 4.3 in our revised manuscript.

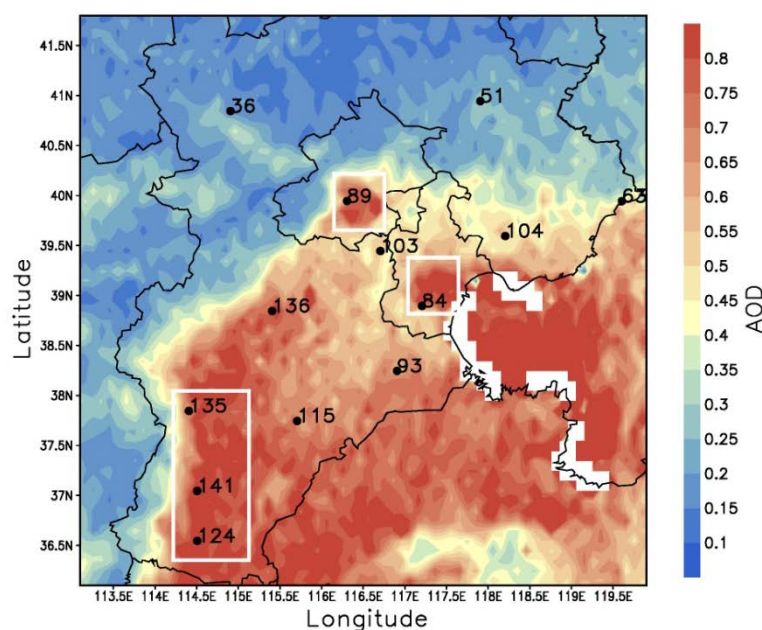


Fig. 4 Distribution of AOD from December 2013 to November 2014 in the NCP. The PM_{2.5} concentrations of the 13 observation sites were also marked beside each station. Major sites in the northern NCP (BJ and TJ) and southern Hebei (SJZ, XT and HD) are enclosed by white rectangles.

Comment 12:

LINE 420-422, although the RH can affect the visibility, it cannot significantly affect the aerosol concentration. Is there any direct physical connections between the high RH conditions and high aerosol concentration?

Response 12:

The RH can not only affect the visibility but also the aerosol concentrations. The direct physical mechanism is the fine particle's hygroscopic growth and the RH has a positive correlation with the fine particle's number and mass concentrations (Hu et al., 2006; Liu et al., 2011; Seinfeld et al., 1998).

Comment 13:

LINE 426-427, "temperature is the main factor in new particle formation," any evidences to support this statement in NCP.

Response 13:

Thank you for your suggestion, and we apologize for this inappropriate illustration. Actually, the temperature has impact on the particles physicochemical reaction rate. The particles' nucleation and other secondary transformation processes are most efficient in a relatively high temperature and RH. If the temperature was lower than the ideal value, the aerosol's secondary transformation processes would be less effective (Seinfeld et al., 1998).

Comment 14:

LINE 437-440, the RH in SJZ is higher than that in TJ (closer to sea), why?

Response 14:

Thank you for your suggestion. The seasonal distributions of near-ground RH from December 2013 to November 2014 in the NCP are depicted in Fig. 5. It is clear that southern Hebei had higher RH values than the northern NCP. The RH distribution was not only related to the distance from the sea but also to the flow fields and synoptic systems. This might resulted from the frequent passage of the Siberian High in the northern NCP, especially in spring and winter. In spring, when frequent sand storms occur, a dry air mass is brought to the northern NCP; thus, the RH in the northern NCP was far less than that in southern Hebei (Fig. 5a). Meanwhile, under the impact of the Siberian High, a frequent weak northwest flow from Inner Mongolia will bring cold and dry air to the northern NCP in winter and autumn, and the north flow was too weak to reach southern Hebei (Su et al., 2004), which will lead to a lower RH in the northern NCP (Fig. 5c and 5d). Additionally, the higher RH in southern Hebei could also be affected by the subtropical high in summer (wet southeast flow from the Yellow Sea) (Fig. 5b).

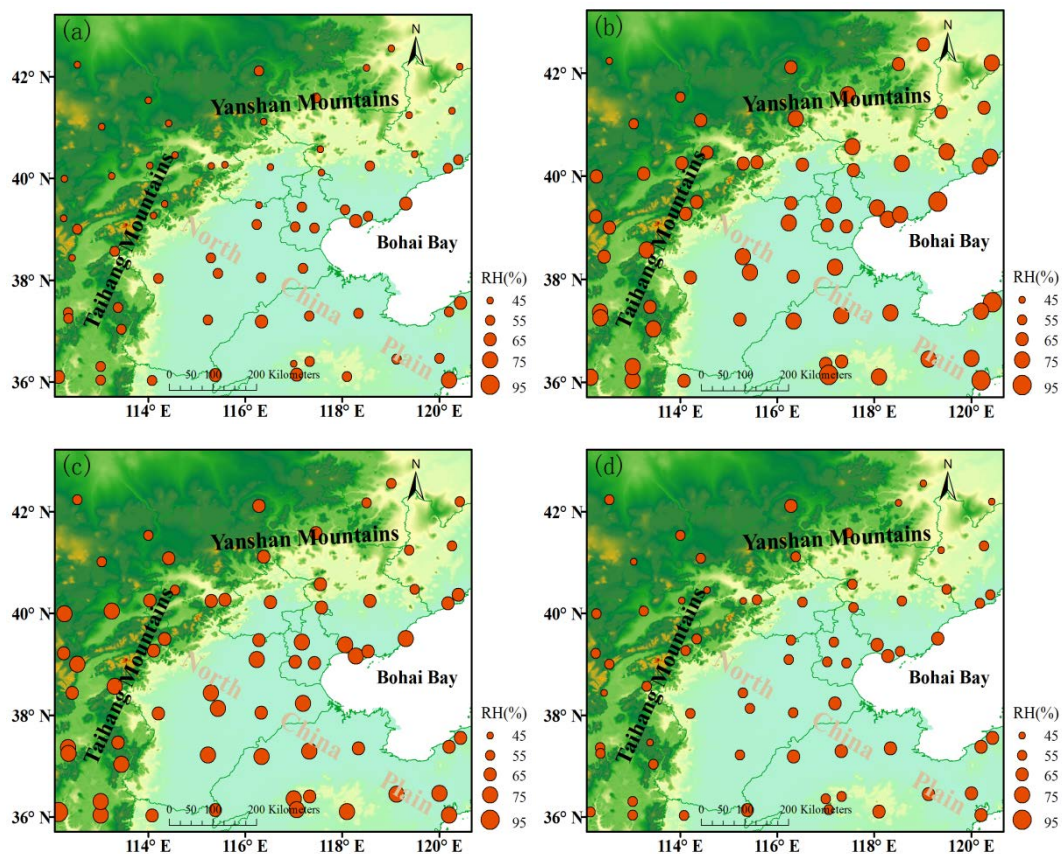


Fig. 5 Distributions of seasonal averaged RH in the NCP from December 2013 to November 2014: (a) spring, (b) summer, (c) autumn and (d) winter.

Comment 15:

Section 4.2.1, the authors attribute the higher PM in SJZ to new particle formation, which is quite complex and cannot be understood merely by the surface temperature and RH. And the direct emissions of pollutants should be considered.

Response 15:

Thank you for your suggestion. Since the particle has direct emissions sources and secondary sources, the distribution of direct emissions cannot represent the total contribution of emissions to the particle concentration. The near-ground $PM_{2.5}$ concentration could represent the particle concentrations at the ground, but considering that the particle lifetime is much longer than that of trace gases, the particle concentrations are nearly uniform in the mixing layer because of strong vertical mixing. Therefore, near-ground $PM_{2.5}$ concentrations cannot be used to evaluate the emissions influences between different regions if the mixing layer heights are different. AOD, which represents the aerosol column concentration, is a much better indicator for the emissions difference. As shown in Fig. 4, the averaged AOD value at southern Hebei (SJZ, HD and XT) was 1.2 times higher than the AOD at the northern NCP (BJ and TJ) region, while the near-ground $PM_{2.5}$ concentration in southern Hebei was 1.5 times higher than that in the northern NCP. If the difference of AOD represents the emissions discrepancy, the remaining differences of the $PM_{2.5}$ concentration may be induced by the meteorology. In other words, except for the

emissions effect, the meteorological conditions also play an important role in pollutant contrast between these two areas. The lower MLH combined with higher RH and weaker wind speed contributed to the heavier haze in southern Hebei. Relevant contents were also modified in section 4.3 in our revised manuscript.

Comment 16:

LINE 470-473, “it was considered reasonable to regard the sounding data of WS as a climatological constant”, during a day, the WS within ML would change due to the momentum exchanges between the ML and free troposphere. The WS cannot be considered as a constant. As illustrated in Fig. S2, there are differences in profiles at 08:00 and 20:00 LT. The error-bar of wind speed should be given.

Response 16:

Thank you for your suggestion, and we apologize for this inaccurate expression. The wind speed in our study was supposed to be a climatological feature, not a climate constant. Additionally, the wind speeds at 08:00 LT and 20:00 LT were used to approximately calculate the ventilation coefficient. Although it will be better to include the sounding data at noon, this is the best choice at present due to the confined acquired data. Relevant contents were supplemented in the conclusion section to explain the uncertainties of our study.

References:

- Hu, M., S. Liu, Z. Wu, J. Zhang, Y. Zhao, W. Birgit, and W. Alfred: Effects of high temperature, high relative humidity and rain process on particle size distributions in the summer of Beijing, *Environ. Sci.*, 27(11), 2006.
- Liu, Z., Y. Sun, L. Li and Y. Wang: Particle mass concentrations and size distribution during and after the Beijing Olympic Games, *Environ. Sci.*, 32(4), doi:10.13227/j.hjcx.2011.04.015, 2011.
- Seinfeld, J. and S. Pandis: *Atmospheric Chemistry and Physics: From Air Pollution to Climate Change*, New York: John Wiley and Sons, 1998.
- Sicard, M., C. Pérez, F. Rocadenbosch, J. Baldasano, and D. García-Vizcaino,: Mixed-Layer Depth Determination in the Barcelona Coastal Area From Regular Lidar Measurements: Methods, Results and Limitations. *Boundary-Layer Meteorology* 119, 135-157, 2006.
- Stull, R.: *An Introduction to Boundary Layer Meteorology*, Kluwer Academic Publishers, Dordrecht, 1988.
- Su, F., M. Yang, J. Zhong, and Z. Zhang: The effects of synoptic type on regional atmospheric contamination in North Chian, *Res. Of Environ. Sci.*, 17(3), doi:10.13198/j.res.2004.03.18.sufq.006, 2004.

Response to comments by referee 3

Specific comments:

The spatial and seasonal characteristics of mixing layer height (MLH) over northern China plain (NCP) were revealed by the authors using variety of measurements, primarily focusing on northern NCP and southern Hebei. The authors attempt to explain the different feature of MLH development between the two interested regions by examining observed wind shear, buoyancy and turbulent stability. In addition, this study pointed out that the MLH plays a key role in forming the heavy near-ground particular mater (PM) pollution besides emissions. The paper is well organized and the reasoning for MLH spatial variations and its association with air pollution is comprehensively discussed. I recommend to publish this paper in ACP journal after addressing following minor issues.

Comment 1:

For Fig. 6: What are the reasons for the difference in buoyancy term profiles between the site XT and BJ during winter, as shown in Fig. 6g? In addition, the absolute values of buoyancy term seem larger than that of shear term; does this mean the buoyancy term rather than the shear term is the dominant component in determining turbulent energy?

Response 1:

Thank you for your suggestion. As we described in section 2.4, the Gradient Richard

number (Ri) is the ratio of buoyancy term $\left(\frac{g}{\theta} \frac{\Delta \bar{\theta}}{\Delta z}\right)$ and shear term $\left(\left(\frac{\Delta \bar{u}}{\Delta z}\right)^2 + \left(\frac{\Delta \bar{v}}{\Delta z}\right)^2\right)$.

For the static instability, the buoyancy term is usually negative, and the buoyancy force will suppress the turbulent development; for the neutral stratification, the buoyancy term is usually zero; and for the static stability stratification, the buoyancy is usually positive, which will promote the turbulent development. While the shear term usually has positive value and attribute to the mechanical turbulence. In our study, the averaged buoyancy term is positive and larger than the shear term, leading to the Ri larger than 1, this indicated that the mechanical production rate can not balance the turbulent kinetic energy's consumption by buoyancy. Therefore, from a statistical point of view, the atmospheric turbulence is stable on the BJ, XT and LT stations. Turbulent energy is affected by various factors, except for the buoyancy term and the mechanical product term, there are also the turbulent transport contribution and the dissipation terms. Through analysis of the Ri value is just for a simplify and effective evaluation. Although the averaged result exhibited a more significant effect of buoyancy term than the shear term, there are many different occasions that the Ri is less than 1, and the shear term may play a dominant role.

As we mentioned in line 407-410, the higher buoyancy term in XT may be resulted from the warm advection from the Loess Plateau. Since the warm advection usually develops from southwest to the northeast and results in strong thermal inversion above the NCP plain, the warm advection will has stronger impact at the XT station than the BJ station. Thus, this will lead to a higher buoyancy term contribution in XT.

Comment 2:

Line 381-382: It appears that the profiles were averaged over only two time points (i.e. 8:00 am and 08:00 pm), right? Can the average of only two time points represent the entire day MLH features which are most significant during noon time?

Response 2:

Thank you for your suggestion. Yes, the profiles were averaged over only two time points (i.e. 8:00 am and 08:00 pm). Analysis of these two time points could explain the lower MLH in XT at 8:00 am and 08:00 pm, but could not exactly illustrate the entire day MLH features. Although we can not better explain the day MLH features with these limited data, our study still provide a fundamental knowledge about the reasons for MLH contrast between northern NCP and southern Hebei. We can also make a prediction about these parameters features during noon time: it is known that the MLH development is mainly affected by the solar radiation during daytime and such radiation is almost consistent on the NCP plain, since the XT has weaker turbulent develop condition (i.e., weaker mechanical force and stronger buoyancy inhibition) than the BJ station, the MLH development at the XT station might be weaker than the BJ station. Such limitation in our study is illustrated in the final paragraph of the conclusion section.

Comment 3:

Line 444-447: In addition to the emission discrepancy and different meteorological factors (like MLH), the aerosol-radiation interactions are a potential candidate to explain different PM pollution between the two interested regions. Therefore, it is better to say 60% is the upper bound of contribution due to meteorological factors.

Response 3:

Thank you for your suggestion. Consider your comment, it is certainly reasonable to say 60 % is the upper bound of contribution due to meteorological factors. Therefore, the relevant contents were modified in section 4.3 in our revised manuscript.

Comment 4:

Line 474: a recent ref should also be cited here:

Wang G, et al. (2016) Persistent sulfate formation from London Fog to Chinese haze. Proceedings of the National Academy of Sciences 113(48):13630-13635.

Response 4:

Thank you for your suggestion. The paper that you mentioned has been cited in our revised manuscript.

Comment 5:

Line 409: “enhance” should be “enhanced” or “enhancement of”.

Response 5:

Thank you for your suggestion. We have already modified the relevant content in the revised manuscript.

Mixing layer height on the North China Plain and meteorological

evidence of serious air pollution in southern Hebei

Xiaowan Zhu^{1,23}, Guiqian Tang^{1,2*}, Jianping Guo³⁴, Bo Hu¹, Tao Song¹, Lili Wang¹,
Jinyuan Xin¹, Wenkang Gao¹, Christoph Münkler⁴⁵, Klaus Schäfer⁵⁶, Xin Li^{1,67}, and
Yuesi Wang¹

¹State Key Laboratory of Atmospheric Boundary Layer Physics and Atmospheric
Chemistry (LAPC), Institute of Atmospheric Physics, Chinese Academy of Sciences,
Beijing 100029, China

~~²Center for Excellence in Regional Atmospheric Environment, Institute of Urban
Environment, Chinese Academy of Sciences, Xiamen 361021, China~~

²³University of Chinese Academy of Sciences, Beijing 100049, China

³⁴State Key Laboratory of Severe Weather & Key Laboratory of Atmospheric
Chemistry of CMA, Chinese Academy of Meteorological Sciences, Beijing 100081,
China

⁴⁵Vaisala GmbH, 22607 Hamburg, Germany

⁵⁶Atmospheric Science College, Chengdu University of Information Technology
(CUIT), Chengdu 610225, China

⁶⁷Beijing Municipal Committee of China Association for Promoting Democracy,
Beijing 100035, China

Correspondence to: G. Tang (tgq@dq.cern.ac.cn)

Abstract

To investigate the spatiotemporal variability of ~~regional the~~ mixing layer height
(MLH) on the North China Plain (NCP), multi-site and long-term observations of ~~the~~
MLH with ceilometers at three inland stations (~~(e.g., Beijing (BJ), Shijiazhuang (SJZ)~~
~~and , Tianjin (TJ))~~) and one coastal site (~~(e.g., Qinhuangdao (QHD))~~) were conducted
from 16 October 2013 to 15 July 2015. The MLH ~~of at~~ the inland stations ~~in~~ the NCP
were highest in summer and lowest in winter, while the MLH ~~in~~ the coastal area of
Bohai was lowest in summer and highest in spring. ~~The regional MLH developed the~~
~~earliest in summer (at approximately 7:00 LT) and reached the highest growth rates~~
~~(164.5 m h⁻¹) at approximately 11:00 LT, while in winter, the regional MLH~~
~~developed much later (at approximately 9:00 LT), with the maximum growth rates~~
~~(101.8 m h⁻¹) occurring at 11:00 LT.~~ As a typical site in southern Hebei, the annual
mean of ~~the~~ MLH at SJZ was 464±183 m, which was 15.0 % and 21.9 % lower than
that at the BJ (594±183 m) and TJ (546±197 m) stations, respectively. Investigation of
~~radiation and the wind shear term and buoyancy term in at~~ the NCP revealed that ~~these~~
~~two parameters in southern Hebei were 2.8 times lower and 1.5 times higher than that~~
~~in northern NCP within 0-1200 m in winter, respectively, leading to a 1.9 the net~~
~~radiation was almost consistent on a regional scale, and the lower MLH in southern~~
~~Hebei was mainly due to the 1.9-2.8-fold higher intensity of wind shear frequency of~~

43 ~~the Gradient Richardson number >1 in southern Hebei compared to~~ ~~than on~~ the
44 northern NCP ~~than in southern Hebei~~ ~~at an altitude of 300–1700 m~~. Furthermore,
45 ~~combined with aerosol optical depth and PM_{2.5} observations, we found that the~~
46 ~~pollutant column concentration contrast (1.2 times) between these two areas was far~~
47 ~~less than the near-ground PM_{2.5} concentration contrast (1.5 times). Through analysis~~
48 ~~of the ventilation coefficient and the relative humidity in southern Hebei were 1.1–2.1~~
49 ~~times smaller and 13.2–22.1 % higher than that on the northern NCP,~~ ~~the~~
50 ~~near-ground heavy pollution in southern Hebei mainly resulted from the lower MLH~~
51 ~~and wind speed, respectively.~~ ~~Therefore~~ ~~As a result, severe haze pollution occurred~~
52 ~~much more readily in southern Hebei and the annual means of near ground PM_{2.5}~~
53 ~~concentrations were almost 1.3 times higher than those of the northern areas.~~ ~~Due~~
54 to the importance of unfavorable weather conditions, ~~industrial capacity should be~~
55 ~~reduced in southern Hebei,~~ heavily polluting enterprises should be relocated, and
56 strong emission reduction measures are required to improve the air quality in southern
57 Hebei.

带格式的：下标

带格式的：下标

58 1. Introduction

59 The convective boundary layer is the region where turbulence is fully developed.
60 The height of the interface where turbulence is discontinuous is usually referred to as
61 the mixing layer height (MLH) (Stull, 1988). The mixing layer is regarded as the link
62 between the near-surface and free atmosphere, and the MLH is one of the major
63 factors affecting the atmospheric dissipation ability, which determines both the
64 volume into which ground-emitted pollutants can disperse, as well as the convective
65 time scales within the mixing layer (Seidel et al., 2010). In addition, continuous MLH
66 observations will be of great importance for the improvement of boundary layer
67 parameterization schemes and for the promotion of meteorological model accuracy.

68 Conventionally, the MLH is usually estimated from radiosonde profiles (Seidel et
69 al., 2010). Although meteorological radiosonde observations can provide high-quality
70 data, they are not suitable for continuous fine-resolution MLH retrievals due to their
71 high cost and limited observation intervals (Seibert et al., 2000). As the most
72 advanced method of MLH detection, remote sensing techniques based on the profile
73 measurements from ground-based instruments such as sodar, radar, or lidar that have
74 the unique vertically resolved observational capability are becoming increasingly
75 popular (Beyrich, 1997; Chen et al., 2001; He et al., 2005). Because sound waves can
76 be easily attenuated in the atmosphere, the vertical range of sodar is generally limited
77 to within 1000 m. However, the optical remote sensing techniques can provide higher
78 height ranges (at least several kilometers). The single-lens ceilometers developed by
79 Vaisala have been widely used in a variety of MLH studies (~~e.g., Alexander et al.,~~
80 ~~2017; Emeis et al., 2004, 2009, 2011; Emeis et al., 2009; Emeis et al., 2011; Eresmaa~~
81 ~~et al., 2006; Munkel et al., 2004, 2007; 2006; Muñoz and Undurraga, 2010; Munkel~~
82 ~~and Rasanen, 2004; Schween et al., 2014; Sokół et al., 2014; Tang et al., 2015, 2016;~~
83 ~~Wagner et al., 2006, 2015; Tang et al., 2015b~~). Compared with other remote sensing
84 instruments, this type of lidar has special features favorable for long-term and
85 multi-station observations (Emeis et al., 2009; Wiegner et al., 2014; Tang et al., 2016),
86 including the low-power system, the eye-safe operation within a near infrared laser

87 band, and the low cost and ease of maintenance during any weather conditions
88 (excluding rainy, strong windy or sandstorm weather conditions) with only regular
89 window cleaning required (Emeis et al., 2004; Tang et al., 2016).

90 The North China Plain (NCP) region is the political, economic and cultural center
91 of China. With the rapid economic development, energy use has increased
92 substantially, resulting in frequent air pollution episodes (e.g., Guo et al., 2011; Li et
93 al., 2013; Liu et al., 2016; Tang et al., 2015a, 2017; Wang et al., 2014; Wang et al.,
94 2013a; Xu et al., 2016; Zhang et al., 2014). The haze pollution has had an adverse
95 impact on human health (Tang et al., 2017a) and has aroused a great deal of concern
96 (Tang et al., 2009; Ji et al., 2012; Zhang et al., 2015a). To achieve the integrated-of
97 development of the Jing-Jin-Ji region, readjustment of the regional industrial structure
98 and layout is imperative. To this end, the industrial capacity of heavily polluting
99 enterprises in the areas with unfavorable weather conditions should be reduced, and
100 these heavily polluting enterprises should be removed to improve the air quality. For
101 the remaining enterprises, the industrial air pollutant emissions structure should be
102 changed, and strong emission reduction measures must be implemented. Although the
103 government has carried out some strategies for joint prevention and control, with the
104 less well-understood distributions of regional weather condition-status on the NCP,
105 how and where to adjust the industrial structures on the NCP are questions in pressing
106 need of answers. As one of the key factors influencing the regional heavy haze
107 pollution (Tang et al., 2012, 2016, 2017b; Quan et al., 2013; Hu et al., 2014; Tang et
108 al., 2016; Zhu et al., 2016; Tang et al., 2017b; Zhang et al., 2016a), the MLH to some
109 extent represents the atmospheric environmental capacity, and the regional
110 distribution and variation of MLH on the NCP can offer a scientific basis for
111 regional industrial distribution readjustment, which will be of great importance for
112 regional haze management.

113 Nevertheless, due to the scarcity of MLH observations on the NCP, reliable and
114 explicit characteristics of MLH on the NCP remain unknown. Tang et al. (2016)
115 utilized the long-term observation data of MLH from ceilometers to analyze the
116 characteristics of MLH variations in Beijing (BJ) and verified the reliability of
117 ceilometers. The results demonstrated that MLH in BJ was high in spring and summer
118 and low in autumn and winter with two transition months in February and September.
119 A multi-station analysis of MLH in the NCP region was conducted in February
120 2014, and the characteristics of high MLH at coastal stations and low MLH at
121 southwest piedmont stations were reported (Li et al., 2015). Miao et al. (2015)
122 modeled the seasonal variations of MLH on the NCP and discovered that the MLH
123 was high in spring due to the strong mechanical forcing and low in winter as a result
124 of the strong thermodynamic stability in the near-surface layer. The mountain-plain
125 breeze and the sea breeze circulations played an important role in the mixing layer
126 process when the background synoptic patterns were weak in summer and autumn
127 (Tang et al., 2016; Wei et al., 2017).

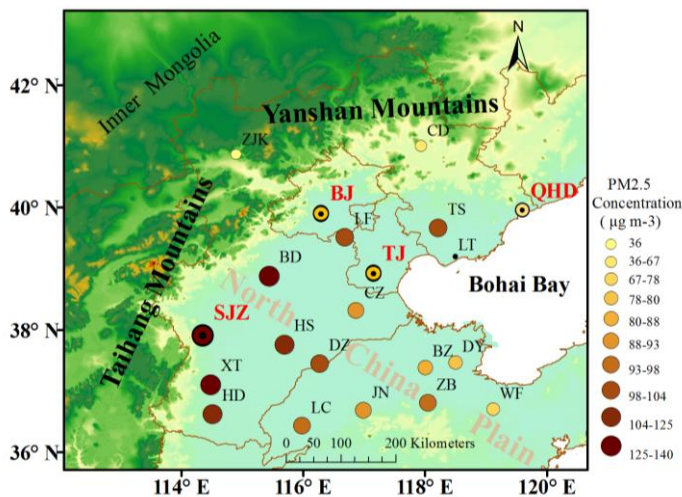
128 However, the regional MLH simulation analysis is incomplete without verification
129 with long term measured MLH data. To overcome previous studies' deficiencies, our
130 study first conducted a 22-months (from 16 October 2013 to 15 July 2015)

131 observation of MLH with ceilometers on the NCP. The observation stations included
 132 three inland stations ~~for example~~ (BJ, Shijiazhuang (SJZ) and Tianjin (TJ)) and one coastal
 133 site ~~for example~~ (Qinhuangdao (QHD)). First, we will describe the spatial and temporal
 134 distribution of MLH on the NCP. Subsequently, reasons for spatial difference of MLH
 135 ~~differences~~ on the NCP will be explained in the discussion section. Finally, ~~the~~ the
 136 meteorological evidence of serious air pollution in southern Hebei will be studied
 137 ~~weather conditions on the NCP are described to provide a scientific basis for regional~~
 138 ~~industrial structure readjustment.~~

139 2 Data and methods

140 2.1 Sites

141 To study the regional MLH characteristics ~~in on~~ the NCP ~~region~~, observations with
 142 ceilometers were conducted at the BJ, SJZ, TJ and QHD stations from 16 October
 143 2013 to 15 July 2015 (Fig. 1 and Table S1). The SJZ, TJ and QHD sites were set
 144 around Beijing in the ~~east southwest~~, southeast and ~~southwest east~~ directions,
 145 respectively. The BJ station was at the base of the Taihang and Yanshan Mountains on
 146 the northern NCP. The MLH observation site was built in the courtyard of the Institute
 147 of Atmospheric Physics, Chinese Academy of Sciences (116.32 ° E, 39.90 ° N). SJZ
 148 was near the Taihang Mountain in southern Hebei; the location was in the Hebei
 149 University of Economics (114.26 ° E, 38.03 ° N). The TJ site was set in the courtyard
 150 of the Tianjin Meteorological Bureau, which was located south of the urban area, with
 151 a geographic location of 117.20 ° E, 39.13 ° N. The QHD station was an eastern coastal
 152 site of Bohai Bay, which was set up in the Environmental Management College of
 153 China (119.57 ° E, 39.95 ° N), and the surrounding areas are mostly residential
 154 buildings with no high structures. Since the TJ site was approximately 50 km away
 155 from the coast and the QHD station was only 2 km, the TJ station, by contrast, was
 156 supposed to be an inland station.



157
 158 Fig. 1- Locations of the ceilometers observation sites (BJ, SJZ, TJ and QHD) were
 159 marked with red and bold abbreviations; other PM_{2.5} observation sites (ZJK, CD, LF,

160 TS, CZ, BD, HS, XT, HD, DZ, LC, JN, BZ, DY, ZB and WF) and the sounding
 161 observation sites (BJ, LT and XT) are marked on the map with black abbreviations.
 162 The size and color of the circular mark are representatives of the annual mean ~~of~~
 163 near-ground PM_{2.5} concentration; the larger and darker the circle is, the greater the
 164 concentration is.

165
 166
 167
 168 **Table 1. Specific information of the observation sites on the NCP.**

Cityname	Abbreviation	Province or municipality	Longitude	Latitude
Beijing ^{a,b,e}	BJ	Beijing	116.32°E	39.90°N
Tianjin ^{a,b}	TJ	Tianjin	117.20°E	39.13°N
Shijiazhuang ^{a,b}	SJZ	Hebei	114.26°E	38.03°N
Langfang ^a	LF	Hebei	116.70°E	39.53°N
Tangshan ^a	TS	Hebei	118.02°E	39.68°N
Qinhuangdao ^{a,b}	QHD	Hebei	119.57°E	39.95°N
Zhangjiakou ^a	ZJK	Hebei	114.92°E	40.90°N
Chengde ^a	CD	Hebei	117.89°E	40.97°N
Laoting ^{b,e}	LT	Hebei	118.90°E	39.31°N
Cangzhou ^a	CZ	Hebei	116.83°E	38.33°N
Baoding ^a	BD	Hebei	115.48°E	38.85°N
Hengshui ^a	HS	Hebei	115.72°E	37.72°N
Xingtai ^{b,e}	XT	Hebei	114.48°E	37.05°N
Handan ^a	HD	Hebei	114.47°E	36.60°N
Dezhou ^a	DZ	Shandong	116.29°E	37.45°N
Liaocheng ^a	LC	Shandong	115.97°E	36.45°N
Jinan ^a	JN	Shandong	116.98°E	36.67°N
Binzhou ^a	BZ	Shandong	118.02°E	37.22°N
Dongying ^a	DY	Shandong	118.49°E	37.46°N
Zibo ^a	ZB	Shandong	118.05°E	36.78°N
Weifang ^a	WF	Shandong	119.06°E	36.68°N

169 ^bNear ground PM_{2.5} concentration sites.

170 ^aCeilmeter observation sites.

171 ^aCeilmeter observation sites.

172 ^bNear ground PM_{2.5} concentration sites.

173 ^cRadiosonde observation sites.

174
 175 **2.2 Measurement of MLH**

176 The instrument used to measure the MLH at the four stations was an enhanced
 177 single-lens ceilometer (Vaisala, Finland), which utilized the strobe laser lidar (laser
 178 detection and range measurement) technique (910 nm) to measure the attenuated
 179 backscattering coefficient profiles. As large differences existed in the aerosol

带格式的：非上标/下标

180 concentrations between the mixing layer and the free atmosphere, the MLH can be
 181 determined from the vertical attenuated backscattering coefficient (β) gradient,
 182 whereby a strong, sudden change in the negative gradient ($-d\beta/dx$) can indicate the
 183 MLH. In the present study, the Vaisala software product BL-VIEW was utilized to
 184 calculate the MLH by determining the location of the maximum ~~$| -d\beta/dx |$~~ ~~$-d\beta/dx$~~
 185 in the attenuated backscattering coefficient. To strengthen the echo signals and reduce
 186 the detection noise, spatial and temporal averaging should be conducted before the
 187 gradient method is used to calculate the MLH. The BL-VIEW software was utilized
 188 with temporal smoothing of 1200 s and vertical distance smoothing of 240 m. The
 189 instrument installed at the BJ station was a CL31 ceilometer and the CL51
 190 ceilometers were used at the SJZ, TJ and QHD stations. Some of the properties of
 191 these two instruments are listed in Table 12, and basic technical descriptions can be
 192 found in M ü nkel et al. (2007) and Tang et al. (2015).

193 To ensure the consistency of the MLH measurements with the two different
 194 ~~versions of~~ ceilometer versions, before we set up the ceilometer observation
 195 networks at different stations in the NCP, we made a comparison of the MLHs
 196 observed by CL31 and CL51 at BJ from October 1 to October 8, 2013 (Fig. S1). The
 197 MLH observed by CL-31 was highly ~~correlated with~~ relevant to those observed by
 198 ~~each of the three~~ CL51 ceilometers, with ~~relative~~ correlation coefficients (R) of
 199 ~~0.9286-0.92, 0.86 and 0.92~~. Therefore, the impact of version discrepancy on the MLH
 200 measurement can be neglected.

201 Since the ceilometers can reflect rainy conditions and the precipitation will
 202 influence the MLH retrieval, the precipitation data were excluded. In addition, a
 203 previous study has compared MLH measurements retrieved from ceilometers and
 204 sounding data (Tang et al., 2016). The results revealed that the ceilometers
 205 underestimates the MLH under neutral conditions caused by strong winds and
 206 overestimate the MLH when sand storms occur. Therefore, data points for these three
 207 special weather conditions were eliminated manually. The criterion to exclude these
 208 data points is as follows: (a) precipitation, i.e., a cloud base lower than 4000 m and
 209 the attenuated backscattering coefficient of at least $2 \times 10^{-6} \text{ m}^{-1} \text{ sr}^{-1}$ within 0 m and the
 210 cloud base, (b) sandstorm, i.e., the ratio of $\text{PM}_{2.5}$ to PM_{10} suddenly decreased to 30 %
 211 or lower and the PM_{10} concentration was higher than $500 \mu\text{g m}^{-3}$, and (c) strong winds,
 212 i.e., a sudden change in temperature and wind speed (WS) when cold fronts passed by
 213 (Muñoz and Undurraga, 2010; Tang et al., 2016; Van der Kamp and McKendry,
 214 2010).

215 Table 12. Instrument properties of CL31 and CL51

Parameter	CL31	CL51
Detection range (km)	7.57	1315.0
Wavelength (nm)	910	910
Report period (s)	2-120	6-120
Report	52m	106m
accuracy Measurement interval (s)		
Peak	310	310

带格式的: 不调整西文与中文之间的空格, 不调整中文和数字之间的空格

带格式的: 字体颜色: 红色

带格式的: 字体颜色: 红色

带格式的: 字体颜色: 红色

带格式的: 字体颜色: 红色

带格式的: 字体颜色: 红色

254 Where Δz is the height increment over which a specific calculation of Ri is being
 255 made; g is the acceleration of gravity; $\bar{\theta}$ is the mean virtual potential temperature
 256 within that height increment; and $\Delta \bar{u}$ and $\Delta \bar{v}$ are the mean wind speeds in zonal and
 257 meridional directions within the height increment.
 258 Using Ri to diagnose turbulence is a classical approach and has been covered in
 259 many textbooks on boundary-layer turbulence (Stull, 1988; Garratt, 1994). It can be
 260 interpreted as the ratio of the buoyancy term $(\frac{g}{\theta} \frac{\Delta \bar{\theta}}{\Delta z})$ to the shear term $(\frac{(\Delta \bar{u})^2}{(\Delta z)^2} +$
 261 $(\frac{\Delta \bar{v}}{\Delta z})^2)$ in the turbulent kinetic equation. When the $Ri > 1$, the turbulence was
 262 suppressed and the mixing layer development will be restrained (Stull, 1988). In our
 263 study, the frequency of $Ri > 1$ was used to represent the atmospheric stability in the
 264 NCP. The larger the frequency is, the more stable turbulent stratification is.

266 3 Results

267 3.1 Frequency distribution of regional MLH

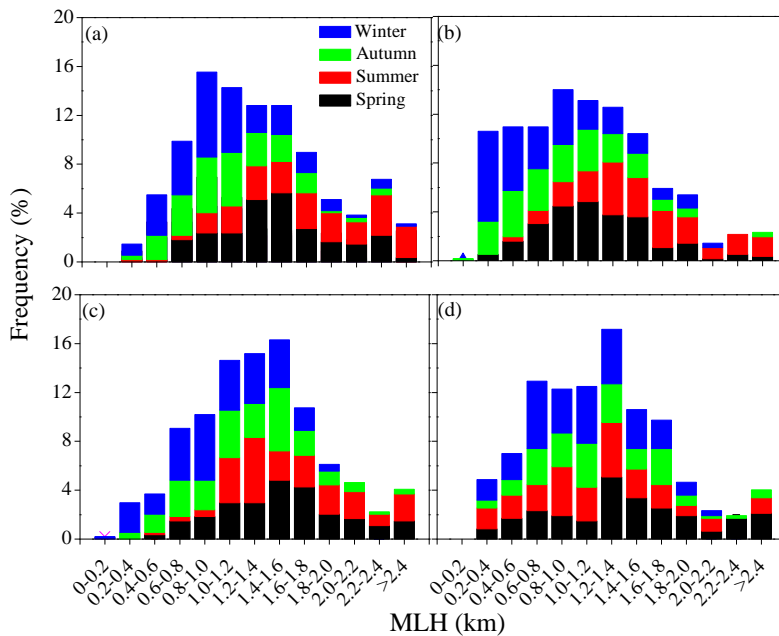
268 Since October 2013, continuous operation of the ceilometers observation network
 269 in the NCP since October 2013 has provided 22 months of MLH data. For the
 270 purpose of analyzing of the MLH temporal and spatial variability variation in the NCP
 271 region, the hourly averages of MLH for a whole year (from December 2013 to
 272 November 2014) at the BJ, SJZ, TJ and QHD stations were utilized chosen in the
 273 following study sections. Hourly means of MLH under rainy, sandstorm and windy
 274 conditions were removed (Muñoz and Undurraga, 2010; Tang et al., 2016; van der
 275 Kamp and McKendry, 2010), resulting in data availability of 81, 89, 83 and 77 % at
 276 the BJ, SJZ, TJ and QHD stations, respectively. The frequency distribution of daily
 277 maximum MLH is shown in Fig. 2. In this study, March, April and May are defined as
 278 spring; June, July and August are defined as summer; September, October and
 279 November are defined as autumn; and December, January and February are defined as
 280 winter.

281 To study the regional distribution characteristic of MLH on the NCP, we analyzed
 282 of the frequency of the daily maximum MLH distribution in Fig. 2. The daily
 283 maximum MLH at the BJ, SJZ and TJ stations reached could reach 2400 m. The
 284 high-large daily maximum values mostly occurred existed in spring and summer,
 285 while the low values always appeared occurred in autumn and winter and were as low
 286 as 200 m. The daily maximum MLH values at the BJ, SJZ and TJ stations were
 287 mainly distributed between 600 and 1800 m, 400 and 1600 m and 800 and 1800 m,
 288 respectively, and they accounted for 74.2, 72.0 and 67.0 % of the total samples,
 289 respectively. Notably, the daily maximum MLH at in SJZ was lower than in spring,
 290 autumn and winter in comparison with those the MLHs at the BJ and TJ stations in

- 带格式的: 字体: (国际) Times New Roman
- 带格式的: 字体: (国际) Times New Roman
- 带格式的: 字体: (国际) Times New Roman
- 带格式的: 字体: Times New Roman
- 带格式的: 字体: (国际) Times New Roman
- 带格式的: 字体: (国际) Times New Roman
- 带格式的: 字体: Times New Roman
- 带格式的: 字体: (国际) Times New Roman
- 带格式的: 字体: (国际) Times New Roman
- 带格式的: 缩进: 首行缩进: 0 厘米
- 带格式的: 字体: 小三, (国际) Times New Roman
- 带格式的: 字体: Times New Roman, 小三
- 带格式的: 字体: Times New Roman, 小三
- 带格式的: 字体: Times New Roman, 小三
- 带格式的: 字体: 小三, (国际) Times New Roman
- 带格式的: 字体: 小三, (国际) Times New Roman
- 带格式的: 字体: 小三, (国际) Times New Roman
- 带格式的: 字体: Times New Roman, 小三
- 带格式的: 字体: 小三, (国际) Times New Roman
- 带格式的: 字体: Times New Roman, 小三
- 带格式的: 字体: 小三, (国际) Times New Roman
- 带格式的: 字体: 小三, (国际) Times New Roman
- 带格式的: 字体: Times New Roman, 小三
- 带格式的
- 带格式的
- 带格式的
- 带格式的
- 带格式的
- 带格式的
- 带格式的: 字体: 非加粗

291 ~~spring, autumn and winter~~. Values below 600 m at the SJZ station occurred primarily
 292 in autumn and winter; ~~t~~. The most frequent daily maximum MLH ~~was existed~~ in the
 293 range ~~of from~~ 1000-~~to~~ 1200 m, which was 200-600 m lower than that at the TJ station.
 294 This ~~pattern~~ demonstrated a weaker atmospheric diffusion capability at ~~the SJZ~~
 295 ~~station~~ in spring, autumn and winter than ~~th at~~ the northern NCP stations.

296 The frequency distribution of the daily maximum MLH at the coastal ~~station-site~~
 297 ~~was showed~~ different ~~features~~. The daily maximum MLH ~~at-in~~ QHD was mainly
 298 distributed between 800 and 1800 m with ~~a~~ relatively ~~uniform-small~~ seasonal
 299 ~~distributions-fluctuation~~ (Fig. 2d). Values lower than 600 m ~~were~~ mainly ~~occurred~~
 300 ~~distributed~~ in summer, which was probably influenced by the frequent occurrence of a
 301 thermal internal boundary layer (TIBL) in summer. ~~(van der Kamp and McKendry,~~
 302 ~~2010)~~. ~~Reasons for this are illustrated in section 4.1.~~



303
 304 Fig. 2. Frequency distribution of ~~the~~ daily maximum MLH at the (a) BJ, (b) SJZ, (c)
 305 TJ and (d) QHD stations from December 2013 to November 2014.

306 3.2 Spatiotemporal variation of ~~regional~~ MLH

307 3.2.1 Seasonal variation

308 Monthly variations of MLH at the BJ, SJZ, TJ and QHD stations are shown in Fig.
 309 3. The monthly means of the regional MLH ranged between 300 and 750 m. ~~T~~;
 310 the maximum and minimum MLH ~~occurred-existed~~ in June 2014 at the BJ station and in
 311 January 2014 at the SJZ station, with values of 741 and 308 m, respectively. Most of
 312 the monthly averages were between 400 and 700 m, which accounted for 81.3 % of
 313 the total samples.

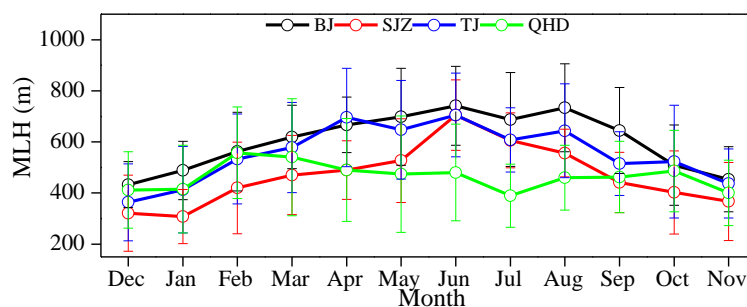
314 The MLH at the BJ, SJZ and TJ stations showed obvious seasonal variations with
 315 high values in spring and summer and low values in autumn and winter. Seasonal
 316 means of MLH at the three stations followed the same order:

317 | summer>spring>autumn>winter, with maximum values of 722 ± 169 , 623 ± 161 and
 318 | 655 ± 165 m in summer, respectively, and minimum values of 493 ± 131 , 347 ± 153 and
 319 | 436 ± 178 m in winter, respectively (Table S2+). Obvious annual changes of the MLH
 320 | with large ~~amplitude values in spring and summer and low values in autumn and~~
 321 | ~~winter~~ at the BJ, SJZ and TJ stations implied that MLH is influenced by seasonal
 322 | changes of solar radiation, ~~and in summer, the intense solar radiation favors the~~
 323 | ~~development of MLH~~ (Stull, 1988).

324 | Nevertheless, the seasonal variation of MLH at the coastal site of Bohai was
 325 | different from that at the inland stations. The MLH ~~at in~~ QHD exhibited a decreasing
 326 | trend from spring to summer and ~~an~~ increasing trend from autumn to winter, ~~and with~~
 327 | the maximum seasonal mean ~~at QHD was of~~ 498 ± 217 m in spring and the minimum
 328 | ~~seasonal mean was of~~ 447 ± 153 m in summer. Moreover, the MLH in spring and
 329 | summer at QHD was much lower than ~~those~~ at other stations. Similar to our analysis
 330 | of frequency distributions of daily maximum MLH in ~~s~~Section 3.1, the lower MLH at
 331 | QHD in spring and summer mainly resulted from the frequent occurrence of ~~the~~
 332 | ~~TIBL sea breeze (Fig. 5). A detailed explanation of the TIBL impact was included in~~
 333 | ~~section 4.1. This-The effect of sea breeze TIBL~~ on the coastal boundary layer was
 334 | consistent with previous studies (Zhang et al., 2013; Tu et al., 2012), which
 335 | demonstrated that ceilometers can properly retrieve the coastal MLH as well.

带格式的: 缩进: 首行缩进: 1 字符

带格式的: 字体颜色: 自动设置



336 |
 337 | Fig. 3 Monthly variations of MLH at the BJ, SJZ, TJ and QHD stations from
 338 | December 2013 to November 2014.

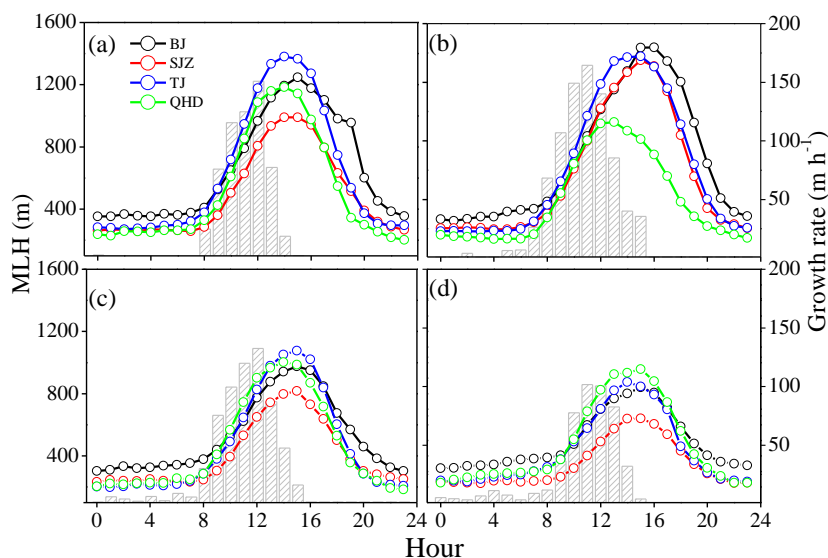
339 | ~~Annual averages of MLH at the BJ, SJZ, TJ and QHD stations were also calculated,~~
 340 | ~~and the values were 594±183, 464±183, 546±197 and 465±175 m, respectively. The~~
 341 | ~~MLH at SJZ was approximately 21.9, 15.0 and 0.2 % lower than at the BJ, TJ and~~
 342 | ~~QHD stations, respectively, which revealed a more stable atmospheric stratification~~
 343 | ~~and weaker atmospheric environment capability in southern Hebei.~~

344 | 3.2.2 Diurnal variations

345 | Seasonal variations of diurnal MLH change patterns were investigated to reveal the
 346 | 24 h evolution characteristics of the ~~regional~~ MLH on the NCP. As shown in Fig. 4,
 347 | diurnal variations of ~~regional~~ MLH in different seasons all had single peak patterns.
 348 | With sunrise and increased solar radiation, MLH at the four stations started to develop
 349 | and peaked in the early afternoon. After sunset, turbulence in the MLH decayed
 350 | quickly, and the mixing layer underwent a transition to the nocturnal stable layer (less
 351 | than 400 m). The ~~averaged~~-annual ~~averaged daily diurnal~~ ranges of MLH at the BJ,

352 SJZ, TJ and QHD stations were 782, 699, 914 and 790 m, respectively, and the
 353 averaged annual averaged diurnal daily range of MLH in at SJZ was approximately
 354 100-200 m smaller than those at the other stations, which was. When we referred to
 355 the diurnal variations of regional MLH in different seasons, we found that the lower
 356 annual daily range at the SJZ station was associated with its lower values of shallow
 357 daytime MLHs in spring, autumn and winter (Figs. 4a, 4c and 4d). This also indicated
 358 the worse pollutant diffusion ability in SJZ.

359 Average growth rates for averaged over the four stations during each season were
 360 plotted with gray columns in Fig. 4. It demonstrated was obvious that the growth rates
 361 of the regional MLH varied by season. The MLH developed the earliest in summer (at
 362 approximately 7:00 LT) and reached the highest growth rates (164.5 m h^{-1}) at
 363 approximately 11:00 LT, and the time when MLH started to develop was found to be
 364 1 hour later (at approximately 8:00 LT) in spring and autumn than in summer.
 365 Furthermore, the MLH developed the latest (at approximately 9:00 LT) and slowest in
 366 winter, with the maximum growth rate (101.8 m h^{-1}) occurring at approximately 11:00
 367 LT.



368
 369 Fig. 4: Diurnal variations of MLH at the BJ, SJZ, TJ and QHD stations in (a) spring,
 370 (b) summer, (c) autumn and (d) winter seasons are indicated by lines and scatters. The
 371 averaged growth rates averaged over at the four sites are depicted drawn with gray
 372 columns for each season to represent the regional MLH growth velocity, and only
 373 positive values are shown in the figure.

374 Considering the MLH peak time and values, we also found that the Comparison of
 375 the MLH peaking time between the four stations showed that the maximum MLH at
 376 the TJ and QHD stations arrived earlier than those at the BJ and SJZ stations in spring
 377 and summer (Figs. 4a and 4b). However, in autumn and winter, such characteristic
 378 was not evident (Figs. 4c and 4d).

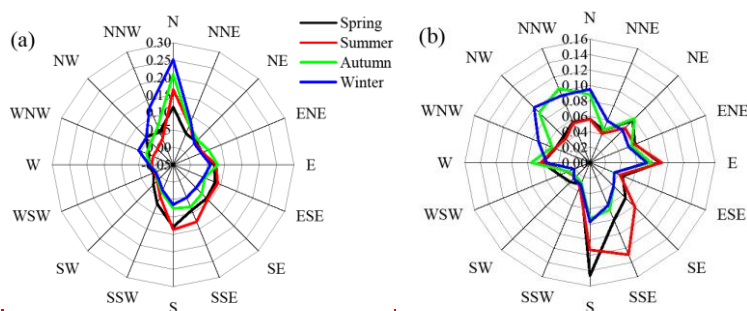
379 When we came to the seasonal wind vectors distribution in the NCP region, we

带格式的：缩进：首行缩进： 1 字
符

380 found that the sea breeze usually started at midday (approximately 11:00 LT) and
381 prevailed during daytime at the QHD station in spring and summer (Fi).

382 As shown in Fig. 5, under the influence of the Siberian High and the geographic
383 location effect, northerly and northwesterly winds prevailed in autumn and winter at
384 the four stations. In spring and summer, the northward lift and westward intrusion of a
385 subtropical high causes the weak southerly wind to arrive and dominate in the NCP
386 region. Without a large or medium scale weather system passing through, the sea
387 breeze will play a role in the coastal area. Although the TJ station was supposed to be
388 an inland site, it was still affected by the sea breeze to some extent. Due to the
389 shoreline orientation and regional topography differences between TJ and QHD (Fig.
390 1), when a sea breeze occurred, easterly wind prevailed at the former station and
391 easterly, and south-southwesterly wind blew at the latter station in spring and summer
392 (Figs.5c and 5d). Statistical results revealed that from March 2014 to August 2014, the
393 frequency of sea breeze occurrence at the TJ and QHD stations could reach 53.8 and
394 92.4 %, respectively, and the sea breeze usually started at midday (approximately
395 11:00 LT).

396 Generally, the vertical development of the mixing layer is heavily reliant on the
397 vertical turbulence, but when sea breeze is present, cool air advection from the sea
398 breeze circulation will suppress this vertical mixing intensity (Puygrenier et al., 2005).
399 The co-existence of vertical turbulence and advection caused the MLH to decrease
400 and peak earlier. Meanwhile, the local mixing layer will be replaced by the thermal
401 internal boundary layer (Tomasi et al., 2011). As a result, the earlier peaking time of
402 MLH in spring and summer could be attributed to the sea breeze effect. The MLH
403 peaking time at the TJ station was approximately 1-2 hours later than at the QHD
404 station, which indicated that such a sea breeze impact will weaken with distance from
405 the coast (Huang et al., 2016).



带格式的: 首行缩进: 0 字符

带格式的:

带格式的: 左, 定义网格后不调整右缩进, 不调整西文与中文之间的空格, 不调整中文和数字之间的空格

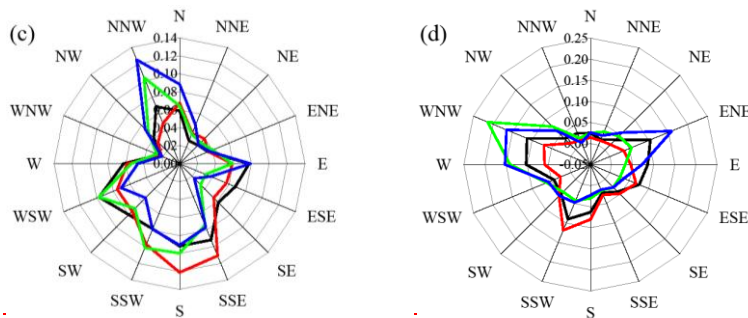


Fig. 5 Frequency of wind direction at the (a) BJ, (b) SJZ, (c) TJ and (d) QHD stations in different seasons.

Annual averages of MLH at the BJ, SJZ, TJ and QHD stations were also calculated, and the values were 594 ± 183 , 464 ± 183 , 546 ± 197 and 465 ± 175 m, respectively. The MLH at SJZ was approximately 21.9, 15.0 and 0.2 % lower than at the BJ, TJ and QHD stations, respectively. Therefore, according to the analysis above in sections 3.1 and 3.2, an obvious phenomenon can be observed in the MLH distribution on the NCP: the MLH in southern Hebei was lower than in the northern NCP in spring, autumn and winter but was almost equal to the northern areas in summer. Annual averages of MLH at the BJ, SJZ, TJ and QHD stations were also calculated, and the values were 594 ± 183 , 464 ± 183 , 546 ± 197 and 465 ± 175 m, respectively. The MLH at SJZ was approximately 21.9, 15.0 and 0.2 % lower than at the BJ, TJ and QHD stations, respectively, which revealed a more stable atmospheric stratification and weaker atmospheric environment capability in southern Hebei. Therefore, according to the analysis above in Sections 3.1 to 3.2, an obvious phenomenon can be observed in the MLH distribution in the NCP region: the MLH was lower in southern Hebei than on the northern NCP in spring, autumn and winter but was almost equal to the northern areas in summer.

4. Discussion

Through preliminary study of the spatiotemporal variation of MLH on the NCP region, we found something interesting: (a) the MLH at the coastal site was lower than the inland sites in summer; (b) the MLH in southern Hebei was lower than the northern NCP in spring, autumn and winter, but was almost consistent between these two areas in summer. Reasons for these two phenomena will be illustrated in the following sections (4.1 and 4.2). Finally, we will investigate the meteorological evidence for serious haze pollution in southern Hebei in section 4.3.

4.1 Reasons for low MLH in southern Hebei: The TIBL impact in coastal site

From the studies in sections 3.1 and 3.2, we found that the maximum MLH at the QHD station was larger and arrived earlier than the BJ, SJZ and TJ stations in summer (Fig. 4b). However, this characteristic was not evident in other seasons (Figs. 4a, 4c and 4d). The sea-land breeze was a local circulation that occurs when there is no large-scale synoptic system passes. In our study, we first excluded days with large-scale synoptic systems. Then, according to the coastline orientation, if the southeast wind at the TJ station and south and southwest winds at the QHD station

带格式的: 缩进: 首行缩进: 1 字符

带格式的: 正文, 无项目符号或编号

带格式的: 字体: (默认) Times New Roman, 小四, 加粗

带格式的: 正文, 无项目符号或编号

带格式的: 字体: (默认) Times New Roman, 小四

带格式的: 字体: (默认) Times New Roman, 小四

带格式的: 字体: (默认) Times New Roman, 小四

带格式的: 字体: (默认) Times New Roman, 小四

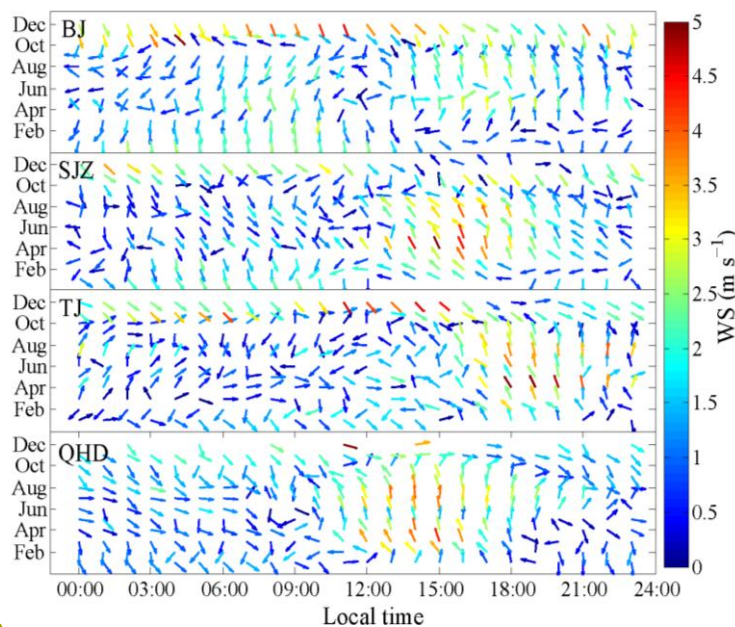
带格式的: 字体: (默认) Times New Roman, 小四

带格式的: 字体: (默认) Times New Roman, 小四

带格式的: 字体: (默认) Times New Roman, 小四

444 occurred at approximately 11:00 LT, and the northwest wind started to blow at
 445 approximately 20:00 LT, then this type of circulation was supposed to be a sea-land
 446 circulation. The prevailing southeast wind at the TJ station and the south and
 447 southwest wind at the QHD station were regarded as sea breezes (Fig. 5).

448 The sea breeze usually brings a cold and stable air mass from the sea to the
 449 coastal region. When the top of the local mixing layer was higher than the top of the
 450 air mass, a TIBL will develop within the mixing layer under the influence of the
 451 abrupt change of aerodynamic roughness and temperature between the land and sea
 452 surfaces. Then, the local mixing layer will be replaced by the TIBL. In the presence of
 453 warm air on land, the cold sea air advects downwind and is warmed, leading to a
 454 weak temperature difference between the air and the ground. In consequence, the
 455 TIBL warms less rapidly due to the decreased heat flux at the ground, and the rise rate
 456 is reduced. In addition, since the TIBL deepens with distance downwind and usually
 457 can not extend all the way to the top of the intruding marine air, the remaining cool
 458 marine air above the TIBL will hinder vertical development of the TIBL (Stull, 1988;
 459 Sicard et al., 2006; Puygrenier et al., 2005; Tomasi et al., 2011). With distance inland,
 460 the top of the intruding marine air will enhance and exceed the local MLH; if so, the
 461 TIBL will not form, and the TIBL impact will be impaired with distance inland (Stull,
 462 1988). Accompanied by the weak synoptic system and the frequent occurrence of sea
 463 breezes in summer, the TIBL formed easily and the MLH peak time and value at the
 464 QHD station were earlier and lower than other stations (Figs. 3 and 4). For the TJ
 465 station, with a distance of approximately 50 km out to sea, the TIBL will not extend
 466 so far. Therefore, although the TJ station can be affected by the sea breeze, the local
 467 MLH cannot be influenced by the TIBL.



468 Fig. 5 Monthly diurnal wind vectors at the BJ, SJZ, TJ and QHD stations from
 469

带格式的: 字体: (默认) Times New Roman, 小四

带格式的: 字体: (默认) Times New Roman, 小四

带格式的: 字体: (默认) Times New Roman, 小四

带格式的: 字体: (默认) Times New Roman, 小四

带格式的: 字体: (默认) Times New Roman, 小四

带格式的: 字体: (默认) Times New Roman, 小四

带格式的: 字体: (默认) Times New Roman, 小四

带格式的: 字体: (默认) Times New Roman, 小四

带格式的: 字体: (默认) Times New Roman, 小四

带格式的: 字体: (默认) Times New Roman, 小四

带格式的: 字体: (默认) Times New Roman, 小四

带格式的: 字体: (默认) Times New Roman, 小四

带格式的: 字体: (默认) Times New Roman, 小四

带格式的: 字体: (默认) Times New Roman, 小四

带格式的: 字体: (默认) Times New Roman, 小四

带格式的: 字体: (默认) Times New Roman, 小四

带格式的: 字体: (默认) Times New Roman, 小四

带格式的: 字体: (默认) Times New Roman, 小四

带格式的: 字体: (默认) Times New Roman, 小四

带格式的: 字体: (默认) Times New Roman, 小四

带格式的: 字体: (默认) Times New Roman, 小四

带格式的: 字体: (默认) Times New Roman, 小四

带格式的: 字体: (默认) Times New Roman, 小四

带格式的: 字体: (默认) Times New Roman, 小四

带格式的: 正文, 居中, 无项目符号或编号

带格式的: 字体: (默认) Times New Roman, 小四

带格式的: 正文, 无项目符号或编号

December 2013 to November 2014.

4.14.2 Reasons for low MLH in southern Hebei

Turbulent energy stability was mainly responsible for the MLH development, and the generation of turbulent energy was highly correlated with the buoyancy heat flux (mainly sensible heat and moisture fluxes) produced by net radiation and the momentum flux caused by wind shear (Stull, 1988). As presented in section 2.4, the Ri could describe the turbulent stability not only from the perspective of thermal forces but also from the perspective of mechanical forces; it was calculated in this section with meteorological sounding profiles to study the reason for MLH differences between southern Hebei and the northern NCP, and the frequency values of $Ri > 1$ were given in this study. With larger frequency comes more stable stratification. Considering the geographic locations (Fig. 1), the lack of sounding data at the SJZ station was replaced by sounding data from the XT station; meanwhile, sounding data from the LT station was used instead of the data from QHD. Each of the four parameter profiles (WS, shear term, buoyancy term, and the frequency of $Ri > 1$) at the BJ, XT and LT stations are depicted in Fig. 6. The profiles were averaged over 8:00 LT and 20:00 LT and vertically smoothed using a 100-m running average to reduce unexpected fluctuations for viewing purposes only. We first compared the net radiation among the BJ, SJZ and TJ observation sites. As shown in Fig. 6, the seasonal net radiation variations were almost consistent among the three stations, and they were high in spring and summer and low in autumn and winter, with annual averages of 5.4, 6.0 and 4.8 $W m^{-2}$, respectively. The comparable net radiation values at the BJ and SJZ stations indicated that the buoyancy flux was unable to explain the MLH differences between the northern NCP and southern Hebei.

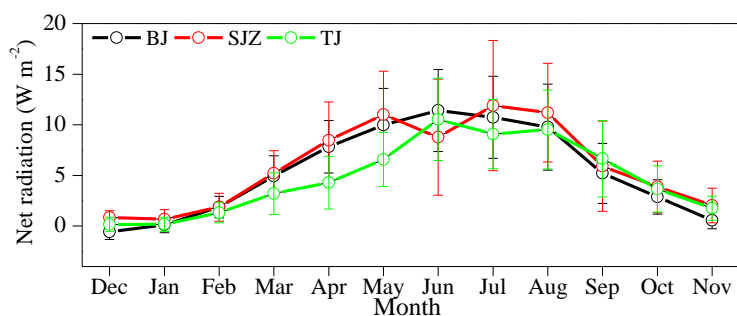


Fig. 6 Monthly variations in net radiation at the BJ, SJZ and TJ sites.

Wind shear was defined and calculated according to Eq. (1):

$$\text{wind shear} = \frac{1}{z_2 - z_1} \left(u_2 - u_1 \right)$$

where z_2 is the height difference between two layers at which the vertical wind shear is estimated and u_2 and u_1 are the differences in zonal and meridional directions in the two different layers (Hyun et al., 2005). Considering the geographic locations (Fig. 1), the lack of sounding data at the SJZ station was addressed by replacement with sounding data from another southern Hebei station (e.g., the XT station); meanwhile, sounding data from another coastal site (e.g., the LT station) were used instead of from the QHD station. Observations were conducted at 8:00 LT and 20:00 LT each day from

带格式的: 字体: (默认) Times New Roman, 小四

带格式的: 字体: 非倾斜

带格式的: 字体: 倾斜

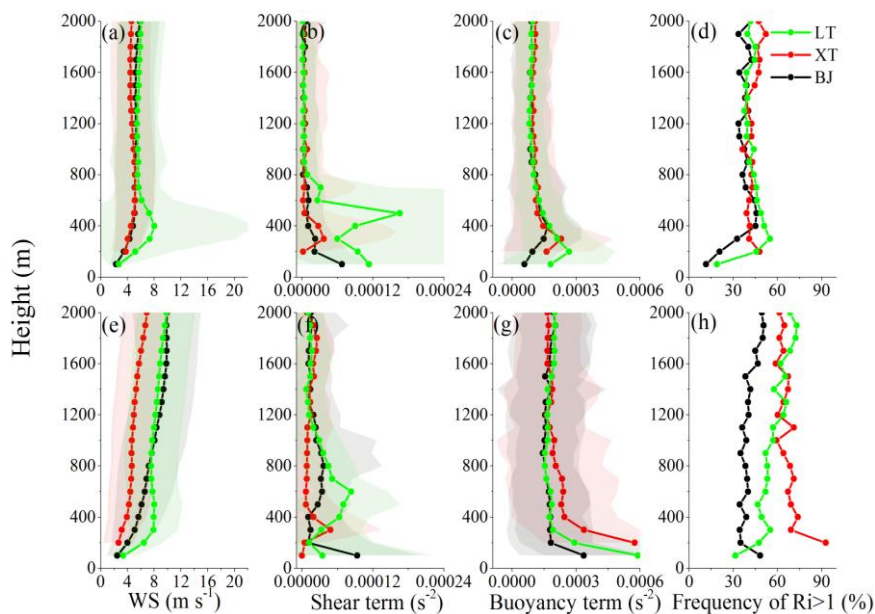
带格式的: 字体: 倾斜

带格式的: 两端对齐, 缩进: 首行缩进: 1 字符

带格式的: 两端对齐, 缩进: 首行缩进: 1 字符

带格式的: 缩进: 首行缩进: 1 字符

505 December 2013 to November 2014, and the wind shear was averaged every 100 m for
 506 each sounding profile.



带格式的：字体：(默认) Times
 New Roman, 小四
 带格式的：居中

507
 508 Fig. 6 Vertical profiles of (a, e) horizontal WS, (b, f) shear term, (c, g) buoyancy term
 509 and (d, h) frequency of $Ri > 1$ at the BJ, XT and LT stations in summer (upper panel)
 510 and winter (lower panel).

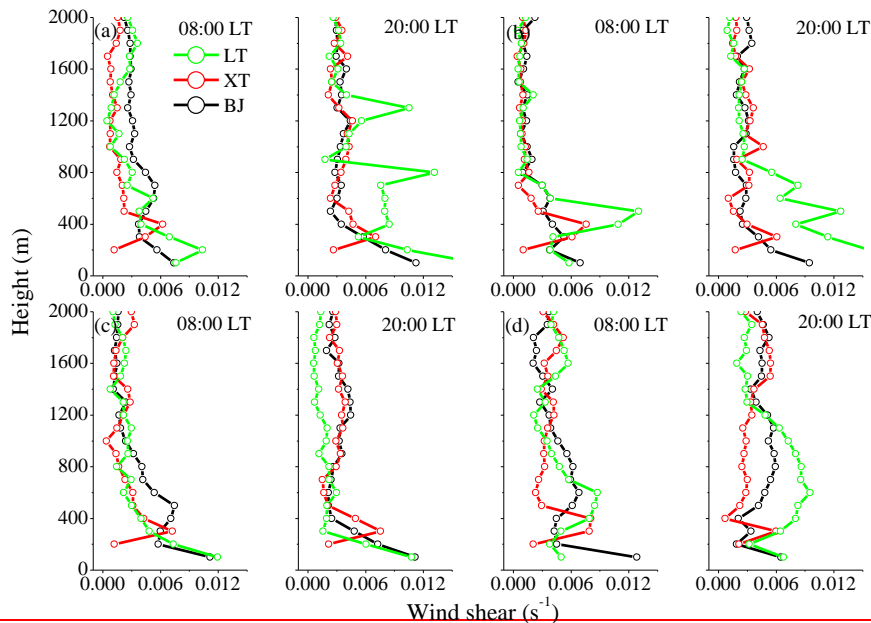
511 ~~Took~~Using the winter and summer as examples, ~~When~~when we analyzed the
 512 seasonal means of ~~wind-shear terms and the buoyancy term~~ between ~~the southern~~
 513 Hebei (XT) and the ~~northern NCP (BJ) stations~~, some distinct features were observed,
 514 ~~As shown in Figs. 6f and 6g.~~ Considering that the regional MLH at 08:00 LT and
 515 20:00 LT was mostly below 300 m in winter (Fig. 4), ~~the wind-shear terms and the~~
 516 ~~buoyancy term in southern Hebei XT were~~ was 2.8 times lower and 1.5 times higher
 517 than ~~those that in the northern NCP BJ within 0-1200 m in winter, respectively, below~~
 518 300 m but were nearly consistent at the altitude of 300 m both at 08:00 LT and 20:00
 519 LT during the whole year. However, above 300 m at 08:00 LT, wind shears at XT
 520 were significantly different from those at BJ again at the altitude of 300-1700 m and,
 521 on average, approximately 2.8, 2.5 and 1.9 times smaller than that at their BJ
 522 stations in spring, autumn and winter, respectively (Figs. 7a, 7c and 7d), and ~~the~~
 523 largest discrepancies of the wind shear term and buoyancy term between southern
 524 Hebei and the northern NCP could reach $2.84 \times 10^{-5} \text{ s}^{-2}$ and $3.4, 4.3, \text{ and } 4.5 \text{ m s}^{-1} \text{ km}^{-1}$
 525 in spring, autumn and winter, respectively, and were at the altitude of between 500 and
 526 7800 m and $3.93 \times 10^{-4} \text{ s}^{-2}$ at 200 m, respectively. As a result, the frequency of $Ri > 1$ in
 527 XT was approximately 3.71.9 times larger than that in BJ within 0-1200 m, leading to
 528 a much more stable stratification in southern Hebei (Fig. 6h). The shear term,
 529 buoyancy term and the frequency of $Ri > 1$ in spring and autumn displayed similar
 530 characteristics to those in winter, and the averaged frequency of $Ri > 1$ in southern

带格式的：字体：倾斜

带格式的：字体：倾斜

带格式的: 字体: 倾斜

531 Hebei was approximately 1.5 and 1.3 times larger than those in northern NCP in
532 spring and autumn, respectively (Fig. S3). While in summer, the averaged differences
533 narrowed down to only 1.2 fold wind shear term, buoyancy term and the
534 frequency of $Ri > 1$ were almost the same between southern Hebei and the northern
535 NCP above 300 m (Figs. 67b, 6c and 6d). Compared to wind shears at 20:00 LT
536 above 300 m in spring, autumn and winter, mechanical forces were clearly enhanced
537 in BJ at the height of 300-1700 m during the whole night and the turbulent energy was
538 restored in the residual layer. With the increase of solar radiation in the morning, the
539 MLH developed and broke through the residual layer. At this time, the combination of
540 buoyancy and wind shear forces will contribute to a higher MLH at BJ during daytime.
541 Furthermore, the larger wind shears below 300 m during night time at the BJ station
542 could partly explain the higher nocturnal boundary layer on the northern NCP (Fig. 4).



543 Fig.7 Vertical profiles of wind shear at the BJ, XT and LT stations in (a) spring, (b)
544 summer, (c) autumn and (d) winter.

546 As a result, the lower MLH in southern Hebei was the result of due to a the more
547 stable atmospheric turbulent structure than the northern NCP lessened mechanical
548 forcing due to wind shear at night than occurred in the northern areas in spring,
549 autumn and winter. This probably resulted from the frequent effect of cold air on the
550 northern NCP, and such cold air was usually too weak to reach southern Hebei (Su et
551 al., 2004). Then the cold front resulting from the cold air system will enhance the
552 wind shear over the northern NCP. In addition, a previous study has revealed that the
553 warm advection from the Loess Plateau usually developed from southwest to
554 northeast, and the higher buoyancy term (Fig. 6g) and lower MLH in southern Hebei
555 will be partially related to the enhanced thermal inversion at the altitude of 1500 m
556 (Hu et al., 2014; Zhu et al., 2016). In summer, due to the northward lift and westward

557 intrusion of the subtropical high on the NCP, the diminishing existence of the weak
558 cold air on the northern NCP accompanied with the regional scale strong solar
559 radiation and strong turbulent activities will lead to a small turbulent stability contrast
560 between southern Hebei and the northern NCP. This pattern could be attributed to the
561 influence of the active fronts passing by under the impact of the Siberian High, and
562 usually, this front system does not reach southern Hebei. In summer, due to the
563 influence of the subtropical high on the NCP and the relatively greater solar radiation,
564 the lessened effects of the front system and strong turbulent exchange will lead to less
565 wind shear contrast in the vertical direction between southern Hebei and the northern
566 NCP.

567 In addition, other researchers proposed that absorbing aerosols above the MLH can
568 be another factor affecting the MLH (Peng et al., 2016; Wang et al., 2013; Li et al.,
569 2016). Absorbing aerosols gives rise to an increasing temperature aloft but a
570 decreasing temperature at the surface, which will enhance the strength of capping
571 inversion and inhibit the convective ability. In contrast, absorbing aerosols within the
572 mixing layer could reduce the capping inversion intensity despite the reduction in the
573 surface buoyancy flux and raise the MLH (Yu et al., 2002). Considering the higher
574 concentrations of surface PM_{2.5} in southern Hebei, absorbing aerosols could have
575 some impacts on MLH development. However, the comprehensive influences from
576 the feedback of absorbing aerosols above and below the MLH are hard to explain
577 without sufficient knowledge of vertical variations in absorbing aerosols at the four
578 stations. Additionally, the mixed state and morphology of absorbing aerosols
579 dominant the absorption effects (Jacobson, 2001; Bond et al., 2013). Therefore,
580 without sufficient observation data, it is difficult to discuss the possible influences of
581 air pollution feedback on MLH development in this study. Elaborate experiments of
582 vertical profiles and the morphology of absorbing aerosols are needed in future
583 studies.

带格式的：缩进：首行缩进：1 字符，定义网格后不调整右缩进，不调整西文与中文之间的空格，不调整中文和数字之间的空格

584 4.24.3 Meteorological evidence of serious air pollution in southern Hebei

585 When we analyzed the near-ground PM_{2.5} and PM₁₀ concentrations distributions on
586 the NCP from December 2013 to November 2014, a unique phenomenon was found
587 and shown in Fig. 1 and Fig. S43. The annual means of near-ground PM_{2.5}
588 concentration in southern Hebei (SJZ, XT, HS, and HD and DZ) was 133.3 124.1 μg
589 m⁻³ (248.8 225.3 μg m⁻³ for the PM₁₀ concentrations), while in the northern areas (BJ,
590 TJ, LF and TJS), it was 86.5 94.9 μg m⁻³ (145.5 126.0 μg m⁻³ for the PM₁₀
591 concentrations), and the difference in the near-ground PM_{2.5} concentration between
592 these two areas can be as high as 1.53-fold (1.51.8-fold for the PM₁₀ concentrations).
593 Since AOD represents the aerosol column concentration, it is a much better indicator
594 for the emissions difference than the PM_{2.5}. Additionally, the averaged annual AOD in
595 southern Hebei was only 1.2 times of that in the northern NCP (Fig. 7). If the
596 difference in AOD represents the emission discrepancy, the remaining differences of
597 PM_{2.5} may be induced by the meteorology. In other words, meteorological conditions
598 may play an important role in pollutants contrast between heavier haze formation in
599 southern Hebei and the meteorological condition contrast between these two areas
600 may contributed at most 60% (considering the aerosol-radiation interactions) to the

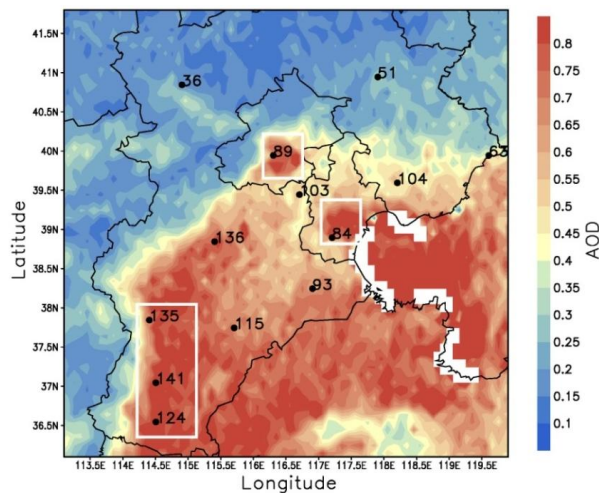
带格式的

带格式的：缩进：首行缩进：1 字符

带格式的：下标

带格式的：下标

601 PM_{2.5} concentration discrepancy. Considering the lower MLH in southern Hebei, the
602 heavily pollution in southern Hebei may be related with weaker weather conditions,
603 and some other meteorological factors may play a part.



带格式的: 字体: (默认) Times
New Roman, 小四

604
605 Fig.7 Distribution of the annual mean values of AOD from December 2013 to
606 November 2014 in the NCP. The PM_{2.5} concentrations of the 13 observation sites
607 were also marked beside each station. The major sites in the northern NCP (BJ and TJ)
608 and southern Hebei (SJZ, XT and HD) are enclosed by white rectangles.

带格式的: 字体颜色: 红色

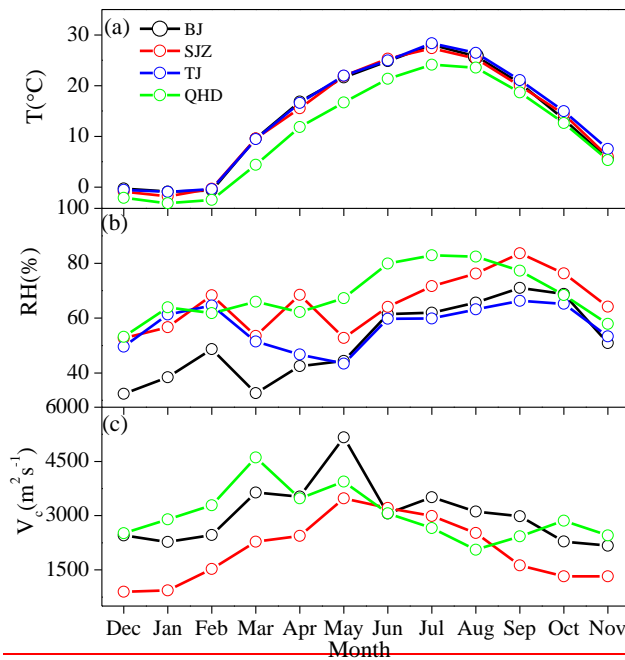
609 Previous studies revealed that the most significant meteorological factors for
610 regional heavy haze formation in the NCP were RH and MLH (Tang et al., 2016;
611 Zhu et al., 2016). In addition, the T influences the particles' physicochemical reaction
612 rate and the ventilation coefficients (V_c) can be used as an index to evaluate the total
613 diffusion ability of the atmosphere; thus, the RH, T and V_c were compared and
614 analyzed among the four stations (BJ, SJZ, TJ and QHD) in the next section. The
615 regional particle growth and the atmospheric dissipation ability will be discussed
616 separately, each from a meteorological point of view. However, due to the lack of
617 wind profiles, Tang et al. (2015) utilized the near-surface WS to estimate the
618 ventilation coefficients (V_c), and the result was not sufficiently precise and could not
619 portray the regional pollution dissipation ability accurately. In this study, we utilized
620 wind sounding data to enable an exact evaluation of the regional pollutant dissipation
621 ability. Furthermore, temperature is the main factor in new particle formation, and RH
622 determines the growth rates of particles, which are the most influential meteorological
623 factors for particle formation. As a consequence, in the next section, we will
624 separately analyze the regional particle formation and dissipation ability, each from a
625 meteorological point of view.

626 4.2.3.1 Meteorological factors for particle formation and growth

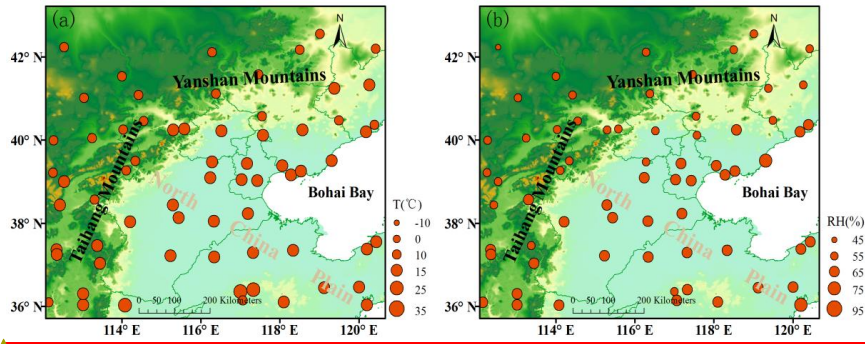
627 Monthly variations Distributions of annual means of T and RH are shown in Fig. 8,
628 and the distributions of seasonal means of T and RH were added in Figs. S5 and Fig.
629 S6-. The T value in the southern Hebei was similar to that on the northern NCP in
630 variation pattern and quantity but was approximately 19.3% higher than that at the

631 coastal site (Figs. 8a and S5). This indicated an almost consistent temperature
 632 condition for an atmospheric physicochemical reaction (Garratt et al., 1994; Tang et al.,
 633 2006; Zhang et al., 2010). Under the same temperature conditions, the new particle
 634 formation ability will be the same between these two areas. However, differences
 635 existed in RH between southern Hebei and the northern NCP. The RH at the SJZ
 636 station was always higher than that at the BJ and TJ stations but was slightly lower
 637 than that at the coastal sites at the QHD station through the year (Figs. 8b and S6).
 638 The annual averages of RH at the BJ, SJZ, TJ and QHD sites were 51.2, 65.7, 57.0
 639 and 68.6 %, respectively, and the RH at SJZ was 22.1 and 13.2 % higher than that
 640 at the BJ and TJ sites, respectively (Table S32). Since RH is also a key factor for
 641 haze development, higher RH is beneficial to fine particle growth through
 642 hygroscopic growth processes and heterogeneous reactions (Zhao et al., 2013; Fu et
 643 al., 2014; Liu et al., 2011; Hu et al., 2006; Wang et al., 2016; Zhang et al., 2015;
 644 Seinfeld et al., 1998), and determines the particle growth rate through hygroscopic
 645 growth and secondary formations (Zhao et al., 2013; Fu et al., 2014), even though the
 646 new particle formation conditions were the same between these two areas, particles
 647 can grow larger under high RH. Thus, a higher RH provided a favorable
 648 meteorological condition for haze development, which could be partially responsible
 649 for heavier pollution in southern Hebei, leading to heavier pollution in southern Hebei.

带格式的: 字体: 非加粗



650



带格式的：字体：(默认) Times New Roman, 小四, 加粗, 字体颜色：文字 1

带格式的：定义网格后不调整右缩进, 不调整西文与中文之间的空格, 不调整中文和数字之间的空格

带格式的：字体：加粗, 字体颜色：文字 1

带格式的：两端对齐

带格式的：下标

651

652 Fig. 8 Distribution of annual means of (a) T and (b) RH in the NCP region from
 653 December 2013 to November 2014.

654 Fig. 8 Seasonal variations of (a) T, (b) RH and (c) V_c at the BJ, SJZ, TJ and QHD
 655 stations from December 2013 to November 2014. The V_c is defined as the product of
 656 MLH to the wind transport (Nair et al., 2007) (Eq. (2)). With larger V_c , strong
 657 dissipation ability follows.

658 **4.23.2 Meteorological factors for particle dissipation**

659 As MLH and WS can represent the atmospheric dissipation capability in the
 660 vertical and horizontal directions, respectively, in addition to the MLH, we ~~also~~
 661 analyzed the WS variations on the NCP. Similar to our analysis in ~~s~~Section 4.21, as
 662 SJZ and QHD had no sounding data and due to the close geographic proximity among
 663 SJZ and XT as well as LT and QHD, sounding data from the XT and LT stations were
 664 used instead of the data at SJZ and QHD, respectively. The WS profiles were
 665 averaged every 100 m at each stations and are depicted in Figs. ~~S26 and S3~~. Except
 666 for summer, the WS in southern Hebei was far less than that on the northern NCP ~~and~~
 667 ~~coastal areas both at 08:00 LT and 20:00 LT~~ in spring, autumn and winter (Figs. ~~6e,~~
 668 ~~S32a, S2e and S3e and S2d~~) but was nearly consistent in summer (Fig. ~~S2b6a~~). This
 669 finding indicated a weaker horizontal diffusion capability in southern Hebei than ~~that~~
 670 on the northern NCP ~~and at the coastal sites~~.

671 The ~~V_c ventilation coefficient~~ is an important factor in pollutant dissipation and air
 672 quality studies; it accounts for the vertical dispersion and advection of pollutants.
 673 With ~~a~~ larger V_c , strong dissipation ability follows. The V_c is defined as the product of
 674 MLH ~~to the~~ ~~and~~ wind transport (U_T) ~~and is as~~ shown in Eq. (2).

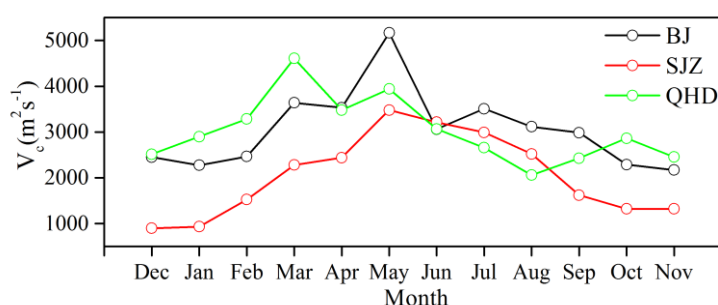
675
$$V_c = MLH \times U_T \quad (2)$$

676 When we utilized the wind profiles in Figs. ~~6 and S3S2~~ with equal spacing in the
 677 vertical direction, U_T could be regarded as the mean wind transport, i.e.,

678
$$U_T = \frac{1}{n} \sum_{i=1}^n U_i U_T =, \text{ and where } U_i \text{ is the wind-WS observed at each level and } n \text{ is the}$$

679 number of levels within the mixing layer (Nair et al., 2007). ~~Since the WS was a~~
 680 ~~climatic parameter, the WS profiles at 08:00 LT and 20:00 LT were used to~~
 681 ~~approximate V_c approximately. As the profiles of WS for each station were almost the~~
 682 ~~same in the morning and at night (Fig. S2), it was considered reasonable to regard the~~
 683 ~~sounding data of WS as a climatological constant, and the V_c within the mixing layer~~

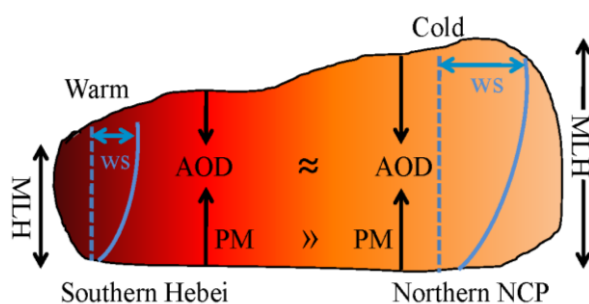
684 ~~could then be calculated.~~ Considering the monthly averaged MLH at the BJ, SJZ and
 685 QHD stations, the monthly V_c ~~is were~~ depicted in Fig. 8e9. V_c at ~~the~~ southern Hebei
 686 was always lower than that in the northern NCP during the whole study period. The
 687 seasonal means of V_c at the BJ, SJZ and QHD stations in spring, summer, autumn and
 688 winter were 4112.0, 2733.3 and 4008.5; 3227.5, 2908.8 and 2593.7; 2481.4, 1421.9
 689 and 2581.7; and 2397.2, 1117.7 and 2900.0 $m^2 s^{-1}$, respectively. It was clear that the
 690 SJZ station usually had the lowest V_c , and the annual averaged V_c at SJZ was almost
 691 1.5 and 1.5 times smaller than the BJ and QHD stations, respectively (Table S32). As
 692 a result, the particle dissipation capability in southern Hebei was much weaker than
 693 that in the northern NCP and coastal areas.



带格式的: 字体: (默认) Times New Roman, 小四

694
 695 Fig. 9 Seasonal variations of V_c at the BJ, SJZ and QHD stations from December
 696 2013 to November 2014. The V_c is defined as the product of MLH and wind transport
 697 (Nair et al., 2007) (Eq. (2)). With a larger V_c , strong dissipation ability follows.

698 Therefore, ~~withdue to the lower atmospheric environment capability~~MLH, lower
 699 ~~WS and higher RH occur~~, ~~the weaker dissipation ability and stronger particle~~
 700 ~~formation ability, the particles were more easily accumulated and severe haze~~
 701 ~~occurred frequently in southern Hebei compared to the northern NCP, the near-ground~~
 702 ~~PM_{2.5} showed a large contrast between these two areas. However, the AOD had little~~
 703 ~~difference between southern Hebei and the northern NCP. Apart from the emission~~
 704 ~~contrast, the meteorological condition contrast between these two areas heavily~~
 705 ~~contributed to the -heavy haze in southern Hebei andthat~~ the industrial structure of
 706 ~~southern Hebei~~ is in need of readjustment for the NCP (Fig. 10).



带格式的: 字体: (默认) Times New Roman, 小四

带格式的: 居中, 首行缩进: 0 字符

707
 708 Fig.10 The schematic diagram of the meteorological causes for heavy haze in
 709 southern Hebei.

带格式的: 左, 缩进: 首行缩进: 0 字符

5. Conclusions

To gain new insight into the spatiotemporal variation of the regional MLH, the present study conducted a simultaneous observation with ceilometers at three inland stations (e.g., BJ, SJZ, and TJ) and one coastal site (e.g., QHD) to obtain high spatial and temporal resolution MLH data. The experiment period lasted for 22-months from October 16, 2013, to July 15, 2015, and one-a whole year's of data (e.g., from December 2013 to November 2014) were utilized for further study. Conclusions were drawn as follows.

The ceilometers can not only retrieve the inland MLH but also retrieve the coastal MLH properly. The MLHs in the inland areas of the NCP was/were high in spring and summer and low in autumn and winter. While under the impact of TIBL, the coastal MLH had an opposite variation trend of inland sites. Under the effects of sea breeze and a thermal internal boundary layer, the seasonal variation of the MLH in the coastal area of Bohai was different from that of the inland stations, and the lowest MLH in QHD was occurred in summer. The TIBL impaired the local MLH development at the coastal site and caused the mixing layer to MLH peaked earlier early at the coastal site in spring and summer than at the inland stations; and this effect weakened with distance from the coast inland. This effect of sea breeze on coastal MLH was consistent with previous studies, which demonstrated that not only can the mainland MLH be retrieved from ceilometers, but the coastal MLH can be observed with ceilometers.

The MLH in southern Hebei was lower than that on the northern NCP, especially in spring, autumn and winter. This As there was little radiation difference between these two areas, the lower MLH in the southern Hebei mainly resulted from the more stable turbulent structure (weak shear term, higher buoyancy term and larger frequency of $Ri > 1$) than stronger intensity of wind shears on the northern NCP, than in southern Hebei at an altitude of 300-1700 m in residual layers, and the stable stratification in southern Hebei was partially related to the Siberian High and warm advection from the Loess Plateau. In summer, the atmospheric stability was almost consistent between southern Hebei and the northern NCP wind shear difference lessened, and the MLHs between the southern and northernese two areas were nearly identicaleonsistent.

From a meteorological point of view, The lower MLH and WS in southern Hebei restricted the atmospheric environmental capability and the pollutant dissipation ability, respectively. weaker atmospheric environment capability Accompanied by combined with the weaker higher RH values pollutant dissipation ability and the stronger pollutant formation ability (stronger pollutant growth ability), the adverse weather conditions will cause severe haze to occur easily in southern Hebei, and the industrial layout in southern Hebei the NCP is in need of restructuring. Heavily polluting enterprises should be relocated to locations with better weather conditions (e.g., certain some northern areas and coastal areas), and strong emission reduction measures should be implemented in the remaining industrial enterprises to improve air quality.

Overall, the present study is the first to conduct a long-term observation of the

带格式的: 字体: 倾斜

754 MLH with high spatial and temporal resolution on a regional scale. The observation
755 results will be of great importance for model parameterization scheme promotion and
756 provide basic information for the distribution of weather conditions in the NCP region.
757 The deficiency of this study is that we ~~took no~~ did not account ~~of~~ for the transport
758 effect on PM_{2.5} concentrations. Because pollutants are usually transported from south
759 to north in the NCP region during haze episodes (Zhu et al., 2016; Tang et al., 2015),
760 ~~the~~ pollutant transport has a greater impact on the northern areas and ~~had~~ has less ~~of~~
761 ~~an~~ influence on the results of this analysis. The absence of sounding data at noon is
762 another shortcoming, and ~~we plan to conduct the~~ daytime observations will be
763 implemented in future experiments. Nevertheless, with the data only at 8:00 LT and
764 20:00 LT, we still provide a fundamental knowledge about the reasons for MLH
765 contrast between northern NCP and southern Hebei, and our study can provide
766 reasonable and scientific suggestions for industrial layout and air pollution emissions
767 reduction measures for the NCP region. ~~This which~~ will be of great importance for
768 achieving the integrated development goals.

769

770 **Acknowledgments**

771 This work was supported by the National Key R&D Program of China
772 (2017YFC0210000), the National Natural Science Foundation of China (41705113),
773 the Beijing Municipal Science and Technology Project (ZL171100000617002) ~~This~~
774 ~~work was supported by the CAS Strategic Priority Research Program (Grant~~
775 ~~no.XDB05020000), the National Natural Science Foundation of China (Grant~~
776 ~~no.41230642)~~ and the National Earth System Science Data Sharing Infrastructure,
777 National Science & Technology Infrastructure of China.

778

779 **References**

780 Beyrich, F.: Mixing height estimation from SODAR data – a critical discussion,
781 Atmos. Environ., 31, 3941–3953, 1997.
782 Bond, T. C., Doherty, S. J., Fahey, D. W., et al.: Bounding the role of black carbon in
783 the climate system: a scientific assessment, J. Geophys. Res., 118, 1-173,
784 doi:10.1002/jgrd.50171, 2013.
785 Chen, W. B., Kuze, H., Uchiyama, A., Suzuki, Y., and Takeuchi, N.: One-year
786 observation of urban mixed layer characteristics at Tsukuba, Japan using a
787 micro pulse lidar, Atmos. Environ., 35, 4273–4280,
788 doi:10.1016/S1352-2310(01)00181-9, 2001.
789 Emeis, S., Münkler, C., Vogt, S., Müller, W. J., and Schäfer, K.: Atmospheric
790 boundary-layer structure from simultaneous SODAR, RASS, and ceilometer
791 measurements, Atmos. Environ., 38(2), 273-286,
792 doi:10.1016/j.atmosenv.2003.09.054, 2004.
793 Emeis, S., Schäfer, K., and Münkler, C.: Observation of the structure of the urban
794 boundary layer with different ceilometers and validation by RASS data,
795 Meteorologische Zeitschrift, 18(2), 149-154, doi:10.1127/0941-2948/2009/0365,
796 2009.
797 Emeis, S., Schäfer, K., Münkler, C., Friedl, R., and Suppan, P.: Evaluation of the

带格式的: 字体: 加粗

798 [Interpretation of Ceilometer Data with RASS and Radiosonde Data,](#)
799 [Bound.-Lay. Meteorol., 143\(1\), 25-35, doi:10.1007/s10546-011-9604-6, 2011.](#)
800 [Eresmaa, N., Karppinen, A., Joffre, S. M., Nen, J. R. S., and Talvitie, H.: Mixing](#)
801 [height determination by ceilometer, Atmos. Chem. Phys., 6, 1485–1493, doi:](#)
802 [10.5194/acp-6-1485-2006, 2006.](#)
803 [Fu, G. Q., Xu, W. Y., Yang, R. F., Li, J. B., and Zhao, C. S.: The distribution and](#)
804 [trends of fog and haze in the North China Plain over the past 30 years, Atmos.](#)
805 [Chem. Phys., 14 \(21\), 11949-11958, 2014.](#)
806 [Garratt, J.: The atmospheric boundary layer. Cambridge University Press, U.K., 316,](#)
807 [1994.](#)
808 [Geiß, A., Wiegner, M., Bonn, B., Schäfer, K., Forkel, R., Schneidmesser, E. V.,](#)
809 [Münkel, C., Chan, K. L., and Nothard, R. Alexander, G., M. Wiegner, B. Bonn,](#)
810 [K. Schäfer, R. Forkel, E. Schneidmesser, C. Münkel, K. Chan, and R. Nothard:](#)
811 [Mixing layer height as an indicator for urban air quality? Atmos. Meas. Tech.,](#)
812 [10, 2969-2988, doi.org/10.5194/amt-10-2969-2017, 2017.](#)
813 [Guo, J. P., Miao, Y., Zhang, Y., Liu, H., Li, Z., Zhang, W., He, J., Lou, M., Yan, Y.,](#)
814 [Bian, L., and Zhai, P.: The climatology of planetary boundary layer height in](#)
815 [China derived from radiosonde and reanalysis data, Atmos. Chem. Phys.,](#)
816 [16\(20\), 13309-13319, doi:10.5194/acp-16-13309-2016, 2016.](#)
817 [Guo, J., Zhang, X., Wu, Y., Che, H., Laba, and Li, X.: Spatio-temporal variation](#)
818 [trends of satellite-based aerosol optical depth in China during 1980-2008,](#)
819 [Atmos. Environ., 45\(37\), 6802-6811,doi: 10.1016/j.atmosenv.2011.03.068,](#)
820 [2011.](#)
821 [He, Q. S., and Mao, J. T.: He, Q. and Mao, J.: Observation of urban mixed layer at](#)
822 [Beijing using a micro pulse lidar, Acta Meteorol. Sin., 63, 374–384, 2005.](#)
823 [Hu, M., Liu, S., Wu, Z. J., Zhang, J., Zhao, Y. L., Wehner, B., and Wiedensolher, A.:](#)
824 [Effects of high temperature, high relative humidity and rain process on particle](#)
825 [size distributions in the summer of Beijing, Environ. Sci., 27\(11\), 2006.](#)
826 [Hu, X. M., Ma, Z. Q., Lin, W. L., Zhang, H. L., Hu, J. L., Wang, Y., Xu, X. B.,](#)
827 [Fuentes, J. D., and Xue, M.: Impact of the Loess Plateau on the atmospheric](#)
828 [boundary layer structure and air quality in the North China Plain?: A case study,](#)
829 [Sci. Total Environ., 499, 228–237, doi:10.1016/j.scitotenv.2014.08.053, 2014.](#)
830 [Jacobson, M. Z.: Strong radiative heating due to the mixing state of black carbon in](#)
831 [atmospheric aerosols, Nature, 409,695-697, 2001.](#)
832 [Ji, D. S., Wang, Y. S., Wang, L. L., Chen, L. F., Hu, B., Tang, G. Q., Xin, J. Y., Song,](#)
833 [T., Wen, T. X., Sun, Y., Pan, Y. P., and Liu, Z. R.: Analysis of heavy pollution](#)
834 [episodes in selected cities of northern China, Atmos. Environ., 50\(2012\),](#)
835 [338-348, 2012.](#)
836 [Jing, T. U., Zhang, S. P., Cheng, X. K., Yang, W. Y., and Yang, Y. Q.: Temporal and](#)
837 [Spatial Variation of Atmospheric Boundary Layer Height\(ABLH\) over the](#)
838 [Yellow East China Sea, J. Ocean U. China, 42\(4\):7-18, 2012.](#)
839 [Kamp, D. V. D., and Mckendry, I.: Diurnal and Seasonal Trends in Convective](#)
840 [Mixed-Layer Heights Estimated from Two Years of Continuous Ceilometer](#)
841 [Observations in Vancouver, BC, Bound.-Lay. Meteorol., 137\(3\), 459-475,](#)

842 [doi:10.1007/s10546-010-9535-7](https://doi.org/10.1007/s10546-010-9535-7), 2010.

843 [Li, M., Tang, G. Q., Huang, X. J., Liu, Z. R., An, J. L., and Wang, Y. S.: Relationship](#)
844 [between atmospheric MLH and winter haze pollution in the Jing-Jin-Ji region,](#)
845 [Environ. Sci., 2015,\(06\):1935-1943, 2015.](#)

846 [Li, P., Xin, J. Y., Bai, X. P., Wang, Y. S., Wang, S. G., Liu, S. X., and Feng, X. X.:](#)
847 [Observational studies and a statistical early warning of surface ozone pollution](#)
848 [in Tangshan, the largest heavy industry city of North China, Inter. J. Env. Res.](#)
849 [Pub. Heal., 10\(3\), 1048-1061, doi:10.3390/ijerph10031048, 2013.](#)

850 [Li, Z. Q., Lau, W. K., Ramanathan, V. et al.: Aeosol and monsoon climate interactions](#)
851 [over Asia, Rev. Geophys., 54, 886-929, doi:10.1002/2015RG000500, 2016.](#)

852 [Liu, Z. R., Hu, B., Zhang, J., Yu, Y., and Wang, Y. S.: Characteristics of aerosol size](#)
853 [distributions and chemical compositions during wintertime pollution episodes](#)
854 [in Beijing, Atmos. Res., 168, 1-12, doi:10.1016/j.atmosres.2015.08.013, 2016.](#)

855 [Liu, Z. R., Sun, Y., Li, L., and Wang, Y. S.: Particle mass concentrations and size](#)
856 [distribution during and after the Beijing Olympic Games, Environ. Sci., 32\(4\),](#)
857 [doi:10.13227/j.hjcx.2011.04.015, 2011.](#)

858 [Miao, Y. C., Hu, X. M., Liu, S. H., Qian, T. T., Xue, M., Zheng, Y. J., and Wang, S.:](#)
859 [Seasonal variation of local atmospheric circulations and boundary layer](#)
860 [structure in the Beijing-Tianjin-Hebei region and implications for air quality, J.](#)
861 [Adv. Model. Earth. Sy., 7\(4\), 1602-1626, doi:10.1002/2015ms000522, 2015.](#)

862 [Münkel, C., and Räsänen, J.: New optical concept for commercial lidar ceilometers](#)
863 [scanning the boundary layer, P.SPIE, 5571, 364-374, 2004.](#)

864 [Münkel, C., Eresmaa, N., Räsänen, J., and Karppinen, A.: Retrieval of mixing height](#)
865 [and dust concentration with lidar ceilometer, Bound.-Lay. Meteorol., 124\(1\),](#)
866 [117-128, doi:10.1007/s10546-006-9103-3, 2007.](#)

867 [Muñoz, R. C., and Undurraga, A. A.: Daytime Mixing layer over the Santiago Basin:](#)
868 [Description of Two Years of Observations with a Lidar Ceilometer, J. Appl.](#)
869 [Meteorol. Clim., 49\(8\), 1728-1741, doi:10.1175/2010jamc2347.1, 2010.](#)

870 [Nair, V. S., Moorthy, K. K., and Alappattu, D. P. et al.: Wintertime aerosol](#)
871 [characteristics over the Indo-Gangetic Plain \(IGP\): Impacts of local boundary](#)
872 [layer processes and long-rang transport, J. Geo. Res.: 2006JD008099,](#)
873 [doi:10.1029/2006JD008099, 2007.](#)

874 [Peng, J. F., Hu, M., Guo, S., Du, Z. F., Zheng, J., Shang, D. J., Misti, L. Z., Zeng, L.](#)
875 [M., Shao, M., Wu, Y. S., Zheng, J., Wang, Y., Glen, C. R., Collins, D. R., and](#)
876 [Molina, M. J.: Markedly enhanced absorption and direct radiative forcing of](#)
877 [black carbon under polluted urban environments, P. Natl. Acad. Sci. Usa.,](#)
878 [113\(4266-4271\), doi:10.1073/pnas.1602310113, 2016.](#)

879 [Puygrenier, V., F. Lohou, B. Campistron, F. Saïl, G. Pigeon, B. Bénéch, and D. Serça:](#)
880 [Investigation on the fine structure of sea-breeze during ESCOMPTE](#)
881 [experiment, Atmos. Res., 74\(1-4\), 329-353,](#)
882 [doi:http://dx.doi.org/10.1016/j.atmosres.2004.06.011, 2005.](#)

883 [Quan, J. N., Gao, Y., Zhang, Q., Tie, X. X., Cao, J. J., Han, S. Q., Meng, J. W., Chen,](#)
884 [P. F., and Zhao, D. L.: Evolution of planetary boundary layer under different](#)
885 [weather conditions, and its impact on aerosol concentrations, Particuology, 11,](#)

886 [34–40, doi:10.1016/j.partic.2012.04.005, 2013.](#)

887 [Schween, J. H., Hirsikko, A., Löhnert, U., and Crewell, S.: Mixing-layer height](#)

888 [retrieval with ceilometer and Doppler lidar: from case studies to long-term](#)

889 [assessment, Atmos. Meas. Tech., 7\(11\), 3685-3704,](#)

890 [doi:10.5194/amt-7-3685-2014, 2014.](#)

891 [Seibert, P., Beyrich, F., Gryning, S. E., Joffre, S., Rasmussen, A., and Tercier, P.:](#)

892 [Review and intercomparison of operational methods for the determination of](#)

893 [the mixing height, Atmos. Environ., 34\(7\), 1001-1027,](#)

894 [doi:http://dx.doi.org/10.1016/S1352-2310\(99\)00349-0, 2000.](#)

895 [Seidel, D. J., Ao, C. O., and Li, K.: Estimating climatological planetary boundary](#)

896 [layer heights from radiosonde observations: Comparison of methods and](#)

897 [uncertainty analysis, J. Geophys. Res., 115, D16113,](#)

898 [doi:10.1029/2009JD013680, 2010.](#)

899 [Seinfeld, J., and Pandis, S.: Atmospheric Chemistry and Physics: From Air Pollution](#)

900 [to Climate Change, New York: John Wiley and Sons, 1998.](#)

901 [Sicard, M., Pérez, C., Rocadenbosch, F., Baldasano, J. M., and Garc ía-Vizcaino, D.:](#)

902 [Mixed-Layer Depth Determination in the Barcelona Coastal Area From Regular](#)

903 [Lidar Measurements: Methods, Results and Limitations. Boundary-Layer](#)

904 [Meteorology 119, 135-157, 2006.](#)

905 [Sokół, P., Stachlewska, I. S., Ungureanu, I., and Stefan, S.: Evaluation of the](#)

906 [boundary layer morning transition using the CL-31 ceilometer signals, Acta](#)

907 [Geophys., 62\(2\), doi:10.2478/s11600-013-0158-5, 2014.](#)

908 [Stull, R.: An Introduction to Boundary Layer Meteorology, Kluwer Academic](#)

909 [Publishers, Dordrecht, 1988.](#)

910 [Su, F. Q., Yang, M. Z., Zhong, J. H., and Zhang, Z. G.: The effects of synoptic type on](#)

911 [regional atmospheric contamination in North China, Res. Of Environ. Sci.,](#)

912 [17\(3\), doi:10.13198/j.res.2004.03.18.sufq.006, 2004.](#)

913 [Tang, G. Q., Li, X., Wang, Y. S., and Xin, J. Y.: Surface ozone trend details and](#)

914 [interpretations in Beijing, 2001–2006, Atmos. Chem. Phys., 9, 8813-8823,](#)

915 [doi:10.5194/acp-9-8813-2009, 2009.](#)

916 [Tang, G. Q., Wang, Y. S., Li, X., Ji, D. S., Hsu, S., and Gao, X.: Spatial-temporal](#)

917 [variations in surface ozone in Northern China as observed during 2009–2010](#)

918 [and possible implications for future air quality control strategies, Atmos. Chem.](#)

919 [Phys., 12, 2757-2776, doi:10.5194/acp-12-2757-2012, 2012.](#)

920 [Tang, G. Q., Zhang, J. Q., Zhu, X. W., Song, T., M ünkel, C., Hu, B., Sch äfer, K., Liu,](#)

921 [Z. R., Zhang, J. K., Wang, L. L., Xin, J. Y., Suppan, P., and Wang, Y. S.: Mixing](#)

922 [layer height and its implications for air pollution over Beijing, China, Atmos.](#)

923 [Chem. Phys., 16\(4\), 2459-2475, doi:10.5194/acp-16-2459-2016, 2016.](#)

924 [Tang, G. Q., Zhao, P. S., Wang, Y. H., Gao, W. K., Cheng, M. T., Xin, J. Y., Li, X., and](#)

925 [Wang, Y. S.: Mortality and air pollution in Beijing: the long-term relationship,](#)

926 [Atmos. Environ., 150, 238-243, doi: 10.1016/j.atmosenv.2016.11.045, 2017a.](#)

927 [Tang, G. Q., Zhu, X. W., Hu, B., Xin, J. Y., Wang, L. L., M ünkel, C., Mao, G., and](#)

928 [Wang, Y. S.: Impact of emission controls on air quality in Beijing during APEC](#)

929 [2014: lidar ceilometer observations, Atmos. Chem. Phys., 15\(21\), 12667-12680,](#)

930 [doi:10.5194/acp-15-12667-2015](https://doi.org/10.5194/acp-15-12667-2015), 2015.

931 [Tang, G. Q., Zhu, X. W., Xin, J. Y., Hu, B., Song, T., Sun, Y., Zhang, J. Q., Wang, L.](#)

932 [L., Cheng, M. T., Chao, N., Kong, L. B., Li, X., and Wang, Y. S.: Modelling](#)

933 [study of boundary-layer ozone over northern China - Part I: Ozone budget in](#)

934 [summer. Atmos. Res., 187, 128-137, 2017b.](#)

935 [Tomasi, F. D., Miglietta, M. M., and Perrone, M. R.: a Case Study, Bound.-Lay.](#)

936 [Meteorol., 139:521-541, doi: 10.1007/s10546-011-9592-6, 2011.](#)

937 [Wagner, M., Emeis, S., Freudenthaler, V., Heese, B., Junkermann, W., Münkler, C.,](#)

938 [Schäfer, K., Seefeldner, M., and Vogt, S.: Mixing layer height over Munich,](#)

939 [Germany: Variability and comparisons of different methodologies, J. Geophys.](#)

940 [Res., 111, D13201, doi:10.1029/2005JD006593, 2006.](#)

941 [Wagner, P. and Schäfer, K.: Influence of mixing layer height on air pollutant](#)

942 [concentrations in an urban street canyon, Urban Climate,](#)

943 <http://dx.doi.org/10.1016/j.uclim.2015.11.001>, 2015.

944 [Wang, G. H., Zhang, R. Y., and Gómesz, M. E. et al.: Persistent sulfate formation](#)

945 [from London Fog to Chinese haze, P. Natl. Acad. Sci., 113\(48\):13630-13635,](#)

946 [doi: 10.1073/pnas.1616540113, 2016.](#)

947 [Wang, L. L., Zhang, N., Liu, Z. R., Sun, Y., Ji, D. S., and Wang, Y. S.: The Influence](#)

948 [of Climate Factors, Meteorological Conditions, and Boundary-Layer Structure](#)

949 [on Severe Haze Pollution in the Beijing-Tianjin-Hebei Region during January](#)

950 [2013, Adv. Meteorol., 2014, 1-14, doi:10.1155/2014/685971, 2014.](#)

951 [Wang, Y. S., Yao, L., Wang, L. L., Liu, Z. R., Ji, D. S., Tang, G. Q., Zhang, J. K., Sun,](#)

952 [Y., Hu, B., and Xin, J. Y.: Mechanism for the formation of the January 2013](#)

953 [heavy haze pollution episode over central and eastern China, Sci. China Earth](#)

954 [Sci., 57\(1\), 14-25, doi:10.1007/s11430-013-4773-4, 2013a.](#)

955 [Wang, Y., Khalizov, A., Levy, M., and Zhang, R. Y.: New Directions: Light absorbing](#)

956 [aerosols and their atmospheric impacts, Atmos. Environ., 81, 713-715, doi:](#)

957 [10.1016/j.atmosenv.2013.09.034](http://dx.doi.org/10.1016/j.atmosenv.2013.09.034), 2013b.

958 [Wei, J., Tang, G. Q., Zhu, X. W., Wang, L. L., Liu, Z. R., Cheng, M. T., Münkler, C.,](#)

959 [Li, X., and Wang, Y. S.: Thermal internal boundary layer and its effects on air](#)

960 [pollutants during summer in a coastal city in North China, Journal of](#)

961 [Environmental Sciences, 1001-0742, doi:10.1016/j.jes.2017.11.006, 2017.](#)

962 [Wiegner, M., Madonna, F., Binietoglou, I., Forkel, R., Gasteiger, J., Geiß, A.,](#)

963 [Pappalardo, G., Schäfer, K., and Thomas, W.: What is the benefit of ceilometers](#)

964 [for aerosol remote sensing? An answer from ERALINET, Atmos. Meas. Tech.,](#)

965 [7, 1979-1997, doi: 10.5194/amt-7-1979-2014, 2014.](#)

966 [Xu, R. G., Tang, G. Q., Wang, Y. S., and Tie, X. X: Analysis of a long-term](#)

967 [measurement of air pollutants \(2007-2011\) in North China Plain \(NCP\); Impact](#)

968 [of emission reduction during the Beijing Olympic Games, Chemosphere, 159,](#)

969 [647-658, doi:10.1016/j.chemosphere.2016.06.025, 2016.](#)

970 [Yu, H., Liu, S. C., and Dickinson, R. E.: Radiative effects of aerosols on the evolution](#)

971 [of the atmospheric boundary layer, J. Geo. Res.: Atmos., 107, D12\(4142\),](#)

972 [doi:10.1029/2001JD000754](http://dx.doi.org/10.1029/2001JD000754), 2002.

973 [Zhang, H., Wang, Y., Hu, J., Ying, Q., and Hu, X. M.: Relationships between](#)

974 meteorological parameters and criteria air pollutants in three megacities in
975 China, Environ. Res., 140, 242–254, doi:10.1016/j.envres.2015.04.004, 2015a.
976 Zhang, J. K., Sun, Y., Liu, Z. R., Ji, D. S., Hu, B., Liu, Q., and Wang, Y. S.:
977 Characterization of submicron aerosols during a month of serious pollution in
978 Beijing, 2013, Atmos. Chem. Phys., 14(6), 2887-2903,
979 doi:10.5194/acp-14-2887-2014, 2014.
980 Zhang, Q., Xin, J. Y., Yin, Y., Wang, L. L., and Wang, Y. S.: The Variation and Trends
981 of MODIS C5 & C6 Products' Errors in the Recent Decade over the
982 Background and Urban Areas of North China, Remote Sensing, 8(9), 754,
983 doi:10.3390/rs8090754, 2016b.
984 Zhang, R. Y., Wang, G. H., Guo, S., Zamora, M. L., Ying, Q., Lin, Y., Wang, W. G.,
985 Hu, M., and Wang, Y.: Formation of Urban Fine Particulate Matter, Chem. Rev.,
986 115, 3803-3855, doi: 10.1021/acs.chemrev.5b00067, 2015b.
987 Zhang, R. Y.: Getting to the Critical Nucleus of Aerosol Formation, Science,
988 328(5984), 1366-1367, doi: 10.1126/science.1189732, 2010.
989 Zhang, W. C., Guo, J. P., Miao, Y. C., Liu, H., Zhang, Y., Li, Z. Q., and Zhai, P. M.:
990 Planetary boundary layer height from CALIOP compared to radiosonde over
991 China, Atmos. Chem. Phys., 16, 9951–9963, doi: 10.5194/acp-16-9951-2016,
992 2016a.
993 Zhang, Z. Z., Cai, X. H., Song, Y., Kang, L., Huang, X., and Li, Q. Y.: Temporal and
994 spatial variation of atmospheric boundary layer height over Hainan Island and
995 its adjacent sea areas, Acta. Sci. Nat. Univ. Pekin., 49:83-90, doi:
996 10.13209/j.0479-8023.2013.105, 2013.
997 Zhao, X. J., Zhao, P. S., Xu, J., Meng, W., Pu, W. W., Dong, F., He, D., and Shi, Q. F.:
998 Analysis of a winter regional haze event and its formation mechanism in the
999 North China Plain, Atmos. Chem. Phys., 13 (11), 5685-5696, 2013.
1000 Zhu, X. W., Tang, G. Q., Hu, B., Wang, L. L., Xin, J. Y., Zhang, J. K., Liu, Z. R.,
1001 Münkel, C., and Wang, Y. S.: Regional pollution and its formation mechanism
1002 over North China Plain: A case study with ceilometer observations and model
1003 simulations, J. Geo. Res.: Atmos., 2016JD025730, doi:10.1002/2016JD025730,
1004 2016.
1005 Beyrich, F.: Mixing height estimation from SODAR data — a critical discussion,
1006 Atmos. Environ., 31, 3941–3953, 1997.
1007 Bond, T. C., et al.: Bounding the role of black carbon in the climate system: a
1008 scientific assessment, J. Geophys. Res., 118, 1–173, doi:10.1002/jgrd.50171,
1009 2013.
1010 Chen, W., Kuze, H., Uchiyama, A., Suzuki, Y., and Takeuchi, N.: One year
1011 observation of urban mixed layer characteristics at Tsukuba, Japan using a micro
1012 pulse lidar, Atmos. Environ., 35, 4273–4280,
1013 doi:10.1016/S1352-2310(01)00181-9, 2001.
1014 Emeis, S., C. Münkel, S. Vogt, W. J. Müller, and K. Schäfer: Atmospheric
1015 boundary layer structure from simultaneous SODAR, RASS, and ceilometer
1016 measurements, Atmos. Environ., 38(2), 273–286,
1017 doi:10.1016/j.atmosenv.2003.09.054, 2004.

带格式的：缩进：左侧：0 厘米，
悬挂缩进：2.5 字符，首行缩进：
-2.5 字符

1018 Emeis, S., K. Schäfer, and C. Münkler: Observation of the structure of the urban
1019 boundary layer with different ceilometers and validation by RASS data.
1020 Meteorologische Zeitschrift, 18(2), 149-154, doi:10.1127/0941-2948/2009/0365,
1021 2009.

1022 Emeis, S., K. Schäfer, C. Münkler, R. Friedl, and P. Suppan: Evaluation of the
1023 Interpretation of Ceilometer Data with RASS and Radiosonde Data, Bound. Lay.
1024 Meteorol., 143(1), 25-35, doi:10.1007/s10546-011-9604-6, 2011.

1025 Eresmaa, N., Karppinen, A., Joffe, S. M., Räsänen, J., and Talvitie, H.: Mixing height
1026 determination by ceilometer, Atmos. Chem. Phys., 6, 1485-1493, doi:
1027 10.5194/acp-6-1485-2006, 2006.

1028 Fu, G., W. Xu, R. Yang, J. Li, and C. Zhao: The distribution and trends of fog and
1029 haze in the North China Plain over the past 30 years, Atmos. Chem. Phys., 14
1030 (21), 11949-11958, 2014.

1031 Garratt JR. The atmospheric boundary layer. Cambridge University Press, U.K., 316,
1032 1994.

1033 Guo, J., Y. Miao, Y. Zhang, H. Liu, Z. Li, W. Zhang, J. He, M. Lou, Y. Yan, L. Bian,
1034 and P. Zhai: The climatology of planetary boundary layer height in China derived
1035 from radiosonde and reanalysis data, Atmos. Chem. Phys., 16(20), 13309-13319,
1036 doi:10.5194/acp-16-13309-2016, 2016.

1037 Guo, J.P., X.Y. Zhang, Y.R. Wu, H.Z. Che, Laba, and X. Li: Spatio-temporal variation
1038 trends of satellite-based aerosol optical depth in China during 1980-2008, Atmos.
1039 Environ., 45(37), 6802-6811, doi: 10.1016/j.atmosenv.2011.03.068, 2011.

1040 He, Q. and Mao, J.: Observation of urban mixed layer at Beijing using a micro-pulse
1041 lidar, Acta Meteorol. Sin., 63, 374-384, 2005.

1042 Hu, X., Ma, Z., Lin, W., Zhang, H., Hu, J., Wang, Y., Xu, X., Fuentes, J. D. and Xue,
1043 M.: Impact of the Loess Plateau on the atmospheric boundary layer structure and
1044 air quality in the North China Plain?: A case study, Sci. Total Environ., 499,
1045 228-237, doi:10.1016/j.scitotenv.2014.08.053, 2014.

1046 Jacobson, M. Z.: Strong radiative heating due to the mixing state of black carbon in
1047 atmospheric aerosols, Nature, 409, 695-697, 2001.

1048 Ji, D., Y. Wang, L. Wang, L. Chen, B. Hu, G. Tang, J. Xin, T. Song, T. Wen, Y. Sun, Y.
1049 Pan, Z. Liu: Analysis of heavy pollution episodes in selected cities of northern
1050 China, Atmos. Environ., 50(2012), 338-348, 2012.

1051 Li M., G. Tang, J. Huang, Z. Liu, J. An, and Y. Wang: Relationship between
1052 atmospheric MLH and winter haze pollution in the Jing Jin Ji region, Environ.
1053 Sci., 2015,(06):1935-1943, 2015.

1054 Li, P., J. Xin, X. Bai, Y. Wang, S. Wang, S. Liu, and X. Feng: Observational studies
1055 and a statistical early warning of surface ozone pollution in Tangshan, the largest
1056 heavy industry city of North China, Inter. J. Env. Res. Pub. Heal., 10(3),
1057 1048-1061, doi:10.3390/ijerph10031048, 2013.

1058 Li, Z., et al.: Aerosol and monsoon climate interactions over Asia, Rev. Geophys., 54,
1059 886-929, doi:10.1002/2015RG000500, 2016.

1060 Liu, Z., B. Hu, J. Zhang, Y. Yu, and Y. Wang: Characteristics of aerosol size
1061 distributions and chemical compositions during wintertime pollution episodes in

带格式的: 缩进: 左侧: 0 厘米,
悬挂缩进: 2 字符, 首行缩进: -2
字符

1062 [Beijing, Atmos. Res., 168, 1–12, doi:10.1016/j.atmosres.2015.08.013, 2016.](#)

1063 [Miao, Y., X. M. Hu, S. Liu, T. Qian, M. Xue, Y. Zheng, and S. Wang: Seasonal](#)

1064 [variation of local atmospheric circulations and boundary layer structure in the](#)

1065 [Beijing-Tianjin-Hebei region and implications for air quality, J. Adv. Model.](#)

1066 [Earth. Sy., 7\(4\), 1602–1626, doi:10.1002/2015ms000522, 2015.](#)

1067 [Münkel, C., and J. Räsänen: New optical concept for commercial lidar ceilometers](#)

1068 [scanning the boundary layer, P.SPIE, 5571, 364–374, 2004.](#)

1069 [Münkel, C., N. Eresmaa, J. Räsänen, and A. Karppinen: Retrieval of mixing height](#)

1070 [and dust concentration with lidar ceilometer, Bound. Lay. Meteorol., 124\(1\),](#)

1071 [117–128, doi:10.1007/s10546-006-9103-3, 200.](#)

1072 [Muñoz, R. C., and A. A. Undurraga: Daytime Mixing layer over the Santiago Basin:](#)

1073 [Description of Two Years of Observations with a Lidar Ceilometer, J. Appl.](#)

1074 [Meteorol. Clim., 49\(8\), 1728–1741, doi:10.1175/2010jame2347.1, 2010.](#)

1075 [Peng, J., M. Hu, S. Guo, Z. Du, J. Zheng, D. Shang, M. L. Zamora, L. Zeng, M. Shao,](#)

1076 [Y. Wu, J. Zheng, Y. Wang, C. R. Glen, D. R. Collins, M. J. Molina, and R. Zhang:](#)

1077 [Markedly enhanced absorption and direct radiative forcing of black carbon under](#)

1078 [polluted urban environments, P. Natl. Acad. Sci. Usa., 113\(4266–4271\),](#)

1079 [doi:10.1073/pnas.1602310113, 2016.](#)

1080 [Puygrenier, V., F. Lohou, B. Campistron, F. Saïd, G. Pigeon, B. Bénéch, and D. Serça:](#)

1081 [Investigation on the fine structure of sea breeze during ESCOMPTE experiment,](#)

1082 [Atmos. Res., 74\(1–4\), 329–353,](#)

1083 [doi:http://dx.doi.org/10.1016/j.atmosres.2004.06.011, 2005.](#)

1084 [Quan, J., Gao, Y., Zhang, Q., Tie, X., Cao, J., Han, S., Meng, J., Chen, P., and Zhao,](#)

1085 [D.: Evolution of planetary boundary layer under different weather conditions,](#)

1086 [and its impact on aerosol concentrations, Particuology, 11, 34–40,](#)

1087 [doi:10.1016/j.partic.2012.04.005, 2013.](#)

1088 [Schween, J. H., A. Hirsikko, U. Löhnert, and S. Crewell: Mixing layer height retrieval](#)

1089 [with ceilometer and Doppler lidar: from case studies to long-term assessment,](#)

1090 [Atmos. Meas. Tech., 7\(11\), 3685–3704, doi:10.5194/amt-7-3685-2014, 2014.](#)

1091 [Seibert, P., F. Beyrich, S. E. Gryning, S. Joffre, A. Rasmussen, and P. Tercier: Review](#)

1092 [and intercomparison of operational methods for the determination of the mixing](#)

1093 [height, Atmos. Environ., 34\(7\), 1001–1027,](#)

1094 [doi:http://dx.doi.org/10.1016/S1352-2310\(99\)00349-0, 2000.](#)

1095 [Seidel, D. J., C. O. Ao, and K. Li: Estimating climatological planetary boundary layer](#)

1096 [heights from radiosonde observations: Comparison of methods and uncertainty](#)

1097 [analysis, J. Geophys. Res., 115, D16113, doi:10.1029/2009JD013680, 2010.](#)

1098 [Sicard, M., Pérez, C., Rocadenbosch, F., Baldasano, J.M., and D. Garcá-Vizcaino:](#)

1099 [Mixed Layer Depth Determination in the Barcelona Coastal Area From Regular](#)

1100 [Lidar Measurements: Methods, Results and Limitations. Boundary Layer](#)

1101 [Meteorology 119, 135–157, 2006.](#)

1102 [Sokół, P., I. Stachlewska, I. Ungureanu, and S. Stefan: Evaluation of the boundary](#)

1103 [layer morning transition using the CL-31 ceilometer signals, Acta Geophys.,](#)

1104 [62\(2\), doi:10.2478/s11600-013-0158-5, 2014.](#)

1105 [Stull, R.B.: An Introduction to Boundary Layer Meteorology, Kluwer Academic](#)

带格式的: EndNote Bibliography, 两端对齐, 缩进: 左侧: 0 厘米, 悬挂缩进: 2 字符, 首行缩进: -2 字符, 定义网格后自动调整右缩进, 调整中文与西文文字的间距, 调整中文与数字的间距

1106 Publishers, Dordrecht, 1988.

1107 Su F.Q., M.Z. Yang, J.H. Zhong, Z.G. Zhang: The effects of synoptic type on regional

1108 atmospheric contamination in North Chian, Res. Of Environ. Sci., 17(3),

1109 doi:10.13198/j.res.2004.03.18.sufq.006, 2004.

1110 Tang, G., J. Zhang, X. Zhu, T. Song, C. Munkel, B. Hu, K. Schäfer, Z. Liu, J. Zhang,

1111 L. Wang, J. Xin, P. Suppan, and Y. Wang: Mixing layer height and its

1112 implications for air pollution over Beijing, China, Atmos. Chem. Phys., 16(4),

1113 2459-2475, doi:10.5194/acp-16-2459-2016, 2016.

1114 Tang, G., P. Zhao, Y. Wang, W. Gao, M. Cheng, J. Xin, X. Li, Y. Wang: Mortality and

1115 air pollution in Beijing: the long term relationship. Atmos. Environ., 150,

1116 238-243, doi: 10.1016/j.atmosenv.2016.11.045, 2017a.

1117 Tang, G., X. Li, Y. Wang, J. Xin, and X. Ren: Surface ozone trend details and

1118 interpretations in Beijing, 2001-2006, Atmos. Chem. Phys., 9, 8813-8823,

1119 doi:10.5194/acp-9-8813-2009, 2009.

1120 Tang, G., X. Zhu, B. Hu, J. Xin, L. Wang, C. Munkel, G. Mao, and Y. Wang: Impact

1121 of emission controls on air quality in Beijing during APEC 2014: lidar ceilometer

1122 observations. Atmos. Chem. Phys., 15(21), 12667-12680,

1123 doi:10.5194/acp-15-12667-2015, 2015.

1124 Tang, G., X. Zhu, J. Xin, B. Hu, T. Song, Y. Sun, J. Zhang, L. Wang, M. Cheng, N.

1125 Chao, L. Kong, X. Li, Y. Wang: Modelling study of boundary layer ozone over

1126 northern China—Part I: Ozone budget in summer. Atmos. Res., 187, 128-137,

1127 2017b.

1128 Tang, G., Y. Wang, X. Li, D. Ji, S. Hsu, and X. Gao: Spatial temporal variations in

1129 surface ozone in Northern China as observed during 2009-2010 and possible

1130 implications for future air quality control strategies, Atmos. Chem. Phys., 12,

1131 2757-2776, doi:10.5194/acp-12-2757-2012, 2012.

1132 Tomasi, F. D., M. M. Miglietta, M. R. Perrone: The Growth of the Planetary

1133 Boundary Layer at a Coastal Site: a Case Study, Bound. Lay. Meteorol.,

1134 139:521-541, doi: 10.1007/s10546-011-9592-6, 2011.

1135 Tu J., S. Zhang, X. Cheng, W. Yang, Y. Yang: Temporal and Spatial Variation of

1136 Atmospheric Boundary Layer Height(ABLH) over the Yellow East China Sea, J.

1137 Ocean U. China, 42(4):7-18, 2012.

1138 van der Kamp, D., and I. McKendry: Diurnal and Seasonal Trends in Convective

1139 Mixed Layer Heights Estimated from Two Years of Continuous Ceilometer

1140 Observations in Vancouver, BC, Bound. Lay. Meteorol., 137(3), 459-475,

1141 doi:10.1007/s10546-010-9535-7, 2010.

1142 Vijayakumar S. Nair, K. K. Moorthy, D. P. Alappattu, P. K. Kunhikrishnan, S. George,

1143 P. R. Nair, S. S. Babu, B. Abish, S. K. Satheesh, S. N. Tripathi, K. Niranjan, B. L.

1144 Madhavan, V. Srikant, C. B. S. Dutt, K. V. S. Badarinath, and R. R. Reddy:

1145 Wintertime aerosol characteristics over the Indo Gangetic Plain (IGP): Impacts

1146 of local boundary layer processes and long rang transport, J. Geo. Res.:

1147 2006JD008099, doi:10.1029/2006JD008099, 2007.

1148 Wagner, P., K. Schäfer: Influence of mixing layer height on air pollutant

1149 concentrations in an urban street canyon, Urban Climate,

带格式的: 缩进: 左侧: 0 厘米,
悬挂缩进: 2 字符, 首行缩进: -2
字符

1150 <http://dx.doi.org/10.1016/j.uclim.2015.11.001>, 2015.

1151 [Wang, L., N. Zhang, Z. Liu, Y. Sun, D. Ji, and Y. Wang: The Influence of Climate](#)

1152 [Factors, Meteorological Conditions, and Boundary Layer Structure on Severe](#)

1153 [Haze Pollution in the Beijing-Tianjin-Hebei Region during January 2013, Adv.](#)

1154 [Meteorol., 2014, 1-14, doi:10.1155/2014/685971, 2014.](#)

1155 [Wang, Y., L. Yao, L. Wang, Z. Liu, D. Ji, G. Tang, J. Zhang, Y. Sun, B. Hu, and J. Xin:](#)

1156 [Mechanism for the formation of the January 2013 heavy haze pollution episode](#)

1157 [over central and eastern China, Sci. China Earth Sci., 57\(1\), 14-25,](#)

1158 [doi:10.1007/s11430-013-4773-4, 2013.](#)

1159 [Wang, Y., M. L. Zamora, and R. Zhang: New Directions: Light absorbing aerosols and](#)

1160 [their atmospheric impacts, Atmos. Environ., 81, 713-715, doi:](#)

1161 [10.1016/j.atmosenv.2013.09.034, 2013.](#)

1162 [Wiegner, M., F. Madonna, I. Biniotoglou, R. Forkel, J. Gasteiger, A. Geiß, G.](#)

1163 [Pappalardo, K. Schäfer, and W. Thomas: What is the benefit of ceilometers for](#)

1164 [aerosol remote sensing? An answer from ERALINET, Atmos. Meas. Tech., 7,](#)

1165 [1979-1997, doi: 10.5194/amt 7-1979-2014, 2014.](#)

1166 [Xu, R., G. Tang, Y. Wang, and X. Tie: Analysis of a long-term measurement of air](#)

1167 [pollutants \(2007-2011\) in North China Plain \(NCP\): Impact of emission](#)

1168 [reduction during the Beijing Olympic Games, Chemosphere, 159, 647-658,](#)

1169 [doi:10.1016/j.chemosphere.2016.06.025, 2016.](#)

1170 [Yu, H., S. Liu, and R. Dickinson: Radiative effects of aerosols on the evolution of the](#)

1171 [atmospheric boundary layer, J. Geo. Res.: Atmos., 107, D12\(4142\),](#)

1172 [doi:10.1029/2001JD000754, 2002.Zhang Z., X. Cai, Y. Song, L. Kang, X. Huang,](#)

1173 [Q. Li: Temporal and spatial variation of atmospheric boundary layer height over](#)

1174 [Hainan Island and its adjacent sea areas, Acta. Sci. Nat. Univ. Pekin., 49:83-90,](#)

1175 [doi: 10.13209/j.0479-8023.2013.105, 2013.](#)

1176 [Zhang, H., Y. Wang, J. Hu, Q. Ying, and X. M. Hu: Relationships between](#)

1177 [meteorological parameters and criteria air pollutants in three megacities in China,](#)

1178 [Environ. Res., 140, 242-254, doi:10.1016/j.envres.2015.04.004, 2015.](#)

1179 [Zhang, J. K., Y. Sun, Z. R. Liu, D. S. Ji, B. Hu, Q. Liu, and Y. S. Wang:](#)

1180 [Characterization of submicron aerosols during a month of serious pollution in](#)

1181 [Beijing, 2013, Atmos. Chem. Phys., 14\(6\), 2887-2903,](#)

1182 [doi:10.5194/acp 14-2887-2014, 2014.](#)

1183 [Zhang, R., G. Hui, S. Guo, M. L. Zamora, Q. Ying, Y. Lin, W. Wang, M. Hu, and Y.](#)

1184 [Wang: Formation of Urban Fine Particulate Matter, Chem. Rev., 115, 3803-3855,](#)

1185 [doi: 10.1021/acs.chemrev.5b00067, 2015.](#)

1186 [Zhang, R.: Getting to the Critical Nucleus of Aerosol Formation, Science, 328\(5984\),](#)

1187 [1366-1367, doi: 10.1126/science.1189732, 2010.](#)

1188 [Zhang, W., J. Guo, Y. Miao, H. Liu, Y. Zhang, Z. Li, and P. Zhai: Planetary boundary](#)

1189 [layer height from CALIOP compared to radiosonde over China, Atmos. Chem.](#)

1190 [Phys., 16, 9951-9963, doi: 10.5194/acp 16-9951-2016, 2016.](#)

1191 [Zhao, X., P. Zhao, J. Xu, W. Meng, W. Pu, F. Dong, D. He, and Q. Shi: Analysis of a](#)

1192 [winter regional haze event and its formation mechanism in the North China Plain,](#)

1193 [Atmos. Chem. Phys., 13 \(11\), 5685-5696, 2013.](#)

带格式的: 正文, 左, 缩进: 左侧: 0 厘米, 悬挂缩进: 2.5 字符, 首行缩进: -2.5 字符, 定义网格后不调整右缩进, 不调整西文与中文之间的空格, 不调整中文和数字之间的空格

带格式的: 英语(英国)

带格式的: 缩进: 左侧: 0 厘米, 悬挂缩进: 2 字符, 首行缩进: -2 字符

1194 Zhu, X., G. Tang, B. Hu, L. Wang, J. Xin, J. Zhang, Z. Liu, C. Munkel, and Y. Wang:
 1195 Regional pollution and its formation mechanism over North China Plain: A case
 1196 study with ceilometer observations and model simulations, J. Geo. Res.: Atmos.,
 1197 2016JD025730, doi:10.1002/2016JD025730, 2016.
 1198 Liu Z. R., Y. Sun, L. Li and Y. S. Wang: Particle mass concentrations and size
 1199 distribution during and after the Beijing Olympic Games, Environ. Sci., 32(4),
 1200 doi:10.13227/j.hjlx.2011.04.015, 2011.
 1201 Hu M., S. Liu, Z. J. Wu, J. Zhang, Y. L. Zhao, W. Birgit, and W. Alfred: Effects of
 1202 high temperature, high relative humidity and rain process on particle size
 1203 distributions in the summer of Beijing, Environ. Sci., 27(11), 2006.
 1204
 1205
 1206
 1207
 1208
 1209
 1210
 1211

带格式的：正文，左，定义网格后
 不调整右缩进，不调整西文与中
 文之间的空格，不调整中文和数
 字之间的空格

带格式的

带格式的：缩进：左侧： 0 厘米，
 悬挂缩进： 2 字符， 首行缩进： -2
 字符